AN ANALYSIS OF STEP SERVO MOTOR PERFORMANCE

CHARLES A. OREM
AND
ALFRED SKOLNICK

AN ANALYSIS OF

STEP SERVO MOTOR PERFORMANCE

****

Charles A. Orem

and

Alfred Skolnick

AN ANALYSIS OF

STEP SERVO MOTOR PERFORMANCE

by

Charles A. Orem

Lieutenant, United States Navy

and

Alfred Skolnick

Lieutenant, United States Navy

Submitted in partial fulfillment of
the requirements for the degree of

MASTER OF SCIENCE
IN
ELECTRICAL ENGINEERING

United States Naval Postgraduate School
Monterey, California

1959

AN ANALYSIS OF

STEP SERVO MOTOR PERFORMANCE

by

Charles A. Orem

and

Alfred Skolnick

This work is accepted as fulfilling

the thesis requirements for the degree of

MASTER OF SCIENCE

IN

ELECTRICAL ENGINEERING

from the

United States Naval Postgraduate School

ABSTRACT

The step servo motor is designed to convert a discrete input into a continuous output. Recent advances in miniaturization techniques have permitted the production of stepper motors capable of following program rates on the order of 100 steps per second.

This paper presents an experimental analysis of step servo motor performance, demonstrates that stepper motor transient responses may be predicted with reasonable accuracy using linear, second order theory, and indicates maximum stepping rate capabilities of the Size 11 Stepper Motor for several different programs. Additionally, it is shown that for the Size 11 Stepper Motor, inability to successfully follow a programmed input is attributable primarily to rotor inertia.

The authors wish to express their appreciation to Mr. Charles W. Cox, Lockheed Missiles and Space Division, Sunnyvale, California, for his invaluable technical assistance and to Professor Charles H. Rothauge, Department of Electrical Engineering, U. S. Naval Postgraduate School, Monterey, California, for his encouragement, guidance and suggestions during the investigation.

TABLE OF CONTENTS

LIST OF ILLUSTRATIONS

LIST OF FIGURES

LIST OF FIGURES

TABLE OF SYMBOLS

English Letter Symbols

Symbol	Definition	Units
ABL	Anti-Backlash	none
BL	Backlash	none
C	Capacitance	farads
d/dt (or " $\dot{}$ ")	Total Time Derivative	none
EMF	Electro Motive Force	volts
f	Damping Coefficient	newton-meters/radian/second
i	Instantaneous Current	ampere
J	Polar Moment of Inertia	kilogram-meters^2
K	Proportionality Constant	newton-meters/weber-ampere-radian
K_D	Proportionality Constant	volts/weber/second
K_g	Proportionality Constant	volts/radian/second
L	Inductance	henries
R	Resistance	ohms
s	The La Placian Operator	none
t	Time	seconds
T	Torque	newton-meters
V_g	Generated (or Induced) EMF	volts
V	Input Voltage	volts

Greek Letter Symbols

Symbol	Definition	Units
ζ	Damping Ratio	none
Θ	Angular Displacement	radians
ϕ	Permanent Magnet Flux	webers
ω_n	Natural Angular Frequency	radians/second

Illus. 1 Frontispiece: Step Response of Size 8 Stepper Motor

I

INTRODUCTION

The step servo motor is not a new device. Large step servo motors have been available and in use for many years; however, not until the advent of guided missiles were low-power, small-size step servo motors manufactured in any quantity.

Recent advances in miniaturization and refined manufacturing techniques have produced step servo motors capable of responding to command rates in excess of 100 steps per second. Within the past three years, small step servo motor technology has progressed so significantly that many missile and control system manufacturers have turned to step servo motors for a solution to the pulse integration problem. The Lockheed Missiles and Space Division of the Lockheed Aircraft Corporation is using a step servo motor in the POLARIS Fleet Ballistic Missile. Several companies are investigating the feasibility of using step servo motors in digital computers. In most cases, the motors are used as a means of pulse integration; although shaft positioning, counting and other control system applications are equally feasible.

A primary advantage of the step servo, or stepper, motor is its simplicity. Presently, such motors are available in four sizes: Size 15, Size 11, Size 8 and Size 5. (The size number indicates the outside diameter of the motor casing in tenths of inches.) The usual stepper

motor design incorporates a solid, permanent-magnet rotor. With an arrangement of four stator windings and appropriate circuitry to energize any two of these windings, a resolved flux vector can be caused to assume positions which divide a cross-sectional plane of the motor into four equal quadrants. Sequential energizing of these windings then rotates the flux vector, which in turn causes the rotor to follow, either clockwise or counterclockwise, as directed.

The purpose of this investigation was twofold: (1) to attempt to obtain sufficient experimental data to develop a generalized theory for stepper motor operation, and (2) to attempt to determine the limits of operation of both a Size 11 and a Size 8 stepper motor. Sufficient information was obtained to permit a valid approximation of motor transient performance by means of linear, second order theory. Additionally, it was proved that the upper limit of stepper motor operation is a function of the inertia of the motor rotor, and that, for a Size 11 motor, this upper limit is at a repetition rate of approximately 100 steps per second for the most stringent input program. Operational limit information for the Size 8 motor was of little value since the motor tested was a prototype and did not satisfy appropriate design requirements.

The experimental portion of this investigation was conducted at the Lockheed Missiles and Space Division, Sunnyvale, California, during the period June-July 1959, under the auspices of the XN Flight Controls Department and under the technical direction of Mr. Charles W. Cox.

The authors wish to express their appreciation to the many Lockheed personnel who assisted in the assembly of test equipment, provided timely and valuable advice and showed a consistently high standard of theoretical and technical ability. In particular, the authors wish to thank Mr. Charles W. Cox, without whose engineering experience and intuition certain phases of this investigation would have been extremely difficult, and Professor Charles H. Rothauge, their Thesis Advisor, whose analytical insight and advice was of great assistance.

II

EXPLANATION OF STEPPER MOTOR OPERATION

A stepper motor is a simple device capable of providing the integral of a series of input pulses. The absence of profound and complex operation is a primary virtue of the step servo motor and an understanding of its performance aspects is readily attainable. The motor itself may be considered to be composed of a permanent magnet rotor and a stator coil arrangement which generates flux vectors that divide a cross-sectional plan of the machine into four equal quadrants (see Fig. 1 and Fig. 2). The stator coils are represented schematically as being composed of two winding sets (see outlined box of Fig. 2). Since the stator is center tapped, each set consists of two windings. Thus, for ease of identification the winding sets are classified as the U stator coil and the V stator coil. These are then subdivided, due to the center tapping, into U, $\overline{U}$, and V, $\overline{V}$ windings. As indicated in Fig. 2, the excitation of any given winding will result in the generation of a flux vector as displayed symbolically by dashed vectors in the diagram. It is not difficult to understand, then, that excitation of either U or $\overline{U}$ in conjunction with the simultaneous excitation of V or $\overline{V}$ will result in a resolved flux vector at the 45 degree, 135 degree, 225 degree or 315 degree angular positions; ① , ② , ③ , and ④ respectively of Fig. 2. Thus, if U and $\overline{V}$ are receiving the required excitation, the resolved flux vector is at position ① and the north pole

of the permanent magnet rotor seeks coincidence with the resolved flux field. If the excited winding is switched from $\overline{V}$ to V, with U remaining in an excited state, the resolved flux vector is effectively rotated 90 degrees. This causes an equal rotation of 90 degrees by the permanent magnet rotor and the shaft of the stepper motor.

In order to make practical use of the motor it is necessary to design and build a switching circuit which will provide effectively instantaneous excitation of any particular winding and thus effect desired motor rotation. The design of such a drive circuit follows typical logic circuit techniques. Forward and reverse motion of the rotor is distinguished in the usual manner as defined progressively by the points of a compass. Forward motion will therefore be clockwise (CW) and reverse motion counter-clockwise (CCW) when looking directly at the motor face from which the shaft projects.

Triggering the drive circuit with pulses results in step voltages being applied to the motor stator windings (see Chapter III); forward or reverse rotation of the motor shaft is then obtainable. This is the method which was used by Lockheed. The drive circuit is produced as a printed circuit card carrying the necessary solid-state devices to effect switching (see Illus. 4); the pulse intelligence for forward or reverse rotor motion is brought in on two separate lines, thus precluding any confusion concerning direction commands. The utility of such a device is obvious, for it accepts discrete pulses as an input and produces their integral as

stepper motor shaft position. By suitably linking the motor shaft through a gear train to drive a resolver, a continuous analog signal may be obtained as resolver output which represents the algebraic sum of pulses entering the input side of the logic circuit.

III

EXPLANATION OF LOGIC CIRCUIT OPERATION

A schematic diagram of the logic circuit used in this investigation is presented in Fig. 1. Illus. 4 is a picture of the actual logic card. A detailed explanation of the logic circuit operation is contained in Appendix C. Understanding of the simplified presentation of Fig. 2 is sufficient to insure comprehension of the stepper motor testing approach used in this study.

Referring to Fig. 2, the permanent magnet rotor of the stepper motor will be in position ④ when $\overline{U}$ and $\overline{V}$ are energized. To move in a forward direction the U flipflop must be hit with a forward pulse. This may be verified by tracing the paths formed by the "and" and "or" gates depicted in Fig. 2. Only the U logic circuitry affords a path for a forward pulse when the condition $\overline{U}$ and $\overline{V}$ obtains. Similarly, if a reverse pulse is imposed it will be fed through the V circuitry since only the V logic branch is sensitive to reverse pulses when the $\overline{U}$ and $\overline{V}$ condition holds.

As an example, consider a forward movement with $\overline{U}$ and $\overline{V}$ energized initially and the rotor north pole at position ④. The U flipflop is sensitive to the forward pulse coming in since only the $\overline{FUV}$ "and" gate is in a condition to permit passage of such a pulse. The succeeding "or" gate passes any of the pulses which enter it and the U flipflop will change state. Hence, the condition changes from $\overline{U}$ to U and the final result is

U and $\bar{V}$. But, U and $\bar{V}$ produces a resolved flux vector pointing in the ① direction; it is obvious that forward motion of the rotor occurs as it seeks coincidence with the new magnetic configuration. The change of state experienced by the flipflop must be communicated to the "and" gates in order that they be aware of the specific state of the flipflop and be prepared to direct ensuing forward or reverse commands to the correct branch of the logic matrix. However, this intelligence must not be transmitted so quickly that the "and" gates assume the new condition dictated before the incoming pulse has had sufficient time to decay; i.e. the possibility of falsely triggering the new matrix condition with the tail end of the same pulse which began the sequence, must be avoided. To accomplish this, the intelligence is delayed by a typical RC delay network.

The response of the logic circuit was investigated and results indicated that a modification to the time constant of the flipflop RC coupling circuits was desirable (see Appendix B). The effect of varying the width of the incoming pulses was essentially negligible, since incoming pulses are differentiated by the transformer stage. Increases in pulse width had no effect until the time interval between pulses was effectively reduced to less than one microsecond. Similarly, reduction in pulse width was not noticeable with regard to circuit operation until the pulse approached widths smaller than one microsecond. As indicated in Fig. 1, two direct current power supplies were required for circuit operation: one at +10 volts and the other at -29.5 volts. The effect of varying supply voltage upon

motor performance is discussed in Appendix B and Chapter VI. The word length, i.e. repetition period of each pulse train measured in bits, and thus steady state rest time, was varied and had a negligible effect upon motor performance. Zero initial conditions were insured by using a word length sufficiently long to provide for complete settling of the rotor prior to imposition of the succeeding program. Thus, an indication of initial rotor position was available. As discussed in detail in Appendix B, the original logic circuit design employed power flipflops directly to drive the stepper motor; this had the disadvantage of exposing these flipflops to the induced EMF effects introduced by the motor when the rotor was traveling at high speeds. By hand cranking the motor and viewing the magnitude of the induced voltages which were possible of generation, it was cursorily determined that such induced voltages were having a detrimental effect upon the power flipflops; i.e. effectively imposing false triggers and causing state changes. Since the primary purpose of this investigation was a study of the stepper motor per se it was necessary to provide some fixture which would serve to isolate the motor and its induced EMF effects from the power flipflops without imposing any noticeable response characteristics of its own. This was accomplished by the circuit of Fig. 3. The response of these power gates was checked and it was established that they introduced a negligible amount of delay and could be neglected in the stepper motor analysis. Oscillograph tapes were obtained which demonstrated the satisfactory isolation provided by the power gates; induced EMF effects appeared on

the motor side of the power gates but not on the logic circuit side. The power gates therefore operated as instantaneous relays which permitted motor excitation as a function of the state of the flipflops; thus the flipflops ceased to be "power" flipflops.

IV

ANCILLARY EQUIPMENT

Illus. 2 shows a general panorama of the test area and the test equipment used. Fig. 4 is a wiring diagram of the test assembly. The most logical method of presentation of the various equipments used in the testing is to follow the history of a typical input program.

Referring to Fig. 4, pulses were generated by the Wang Pulse Generator. This pulse generator was capable of producing independent programs of 12 pulses on both the direct and delayed output. During testing, forward pulses were obtained from the direct output and reverse pulses from the delayed output. Variation of pulse width, pulse spacing and delay time between the end of a pulse sequence and the beginning of a succeeding sequence was possible using the face-mounted controls. Pulses so generated passed to the emitter-follower which served as a buffer stage between the vacuum tubes of the pulse generator and the transistors of the logic circuit. From the emitter-follower the pulses proceeded to the logic circuit. This circuit was mounted in the Stepper Motor Drive (Check Out) Fixture (see Illus. 2) which merely served as a means of mounting the logic circuit and permitted rapid connection of leads. From the logic circuit, the voltage steps generated therein passed through the power gate buffer circuit, and on to the motor stator windings. Illus. 3 shows the anti-backlash and standard gear train connections between the Size 11 motors and their respective resolvers.

A comparison of the Size 8 and Size 11 motors is indicated in Illus. 5. Illus. 6 shows the anti-backlash gear train connection between the Size 8 stepper motor and its resolver.

The standard gear train was used only to indicate the considerable improvement in response which results from the use of anti-backlash gearing. The anti-backlash gear train had a gear ratio of 70.6:1. Consequently, the load offered by the gear-train-resolver combination was practically negligible at the stepper motor shaft. This is readily apparent in Fig. 8A which shows the currents in stepper motor stator windings both with the gear-train-resolver load and with no load on the stepper motor; no visible differences exist. Therefore, data obtained with the gear train and resolver connected to the motor shaft truthfully represent the motor response. It will be shown later that significant motor loading causes definite differences in field current traces (see Chap. VI-1).

The resolver field coils were excited with 115 volts, 800 cycles from the Audio Signal Generator (see Illus. 2). This carrier was modulated by the motion of the resolver rotor resulting from stepper motor action; thus, a particular resolver output level corresponded to a specific stepper motor shaft position. Initial stepper motor position was arranged to correspond to approximately resolver null. The modulated output was fed to either or both of the oscilloscopes and the oscillograph. The oscilloscopes used had a rise time of a fraction of one microsecond and

were capable of time resolutions on the order of one microsecond per centimeter.

The oscillograph was capable of 18-channel simultaneous recording; however, a maximum of 5 channels had amplifiers available to them. Resolver output was applied both directly to the light-beam-reflection (mirror) galvonometers of the oscillograph and through the amplifier assembly (see Illus. 8). The response of the oscillograph-amplifier combination is shown in Fig. 5. Since the carrier was at a frequency of 800 cycles per second, it is apparent that the oscillograph response was adequate. For operation of the oscillograph without amplifier, the response will be even better than that indicated in Fig. 5.

Illus. 7 shows the Stepper Motor Acceptance Kluge (the term "Kluge" is used for all test setups or components which have been temporarily constructed for a particular test) which was used as a means of obtaining static torque data on both sizes of motor. Static torques were measured using a torque watch capable of measuring from 0.02 to 2.40 inch-ounces. Both the torque watch and the angular deflection measurement dial were mounted on the stepper motor shaft in a manner to minimize axial unbalance.

V

PLAN OF INVESTIGATION

1. Transient Response.

When all the physical and electrical parameters defining the stepper motor are compiled, certain linearizing assumptions can be made which produce a linear second order differential equation that defines the step servo motor response. The study of empirical stepper motor transient responses had a two-fold purpose. First, it was desirable to show that the experimental response to a step correlated reasonably well with the theoretical response to a step obtained from the linearized transfer function. This, of course, would afford prima facie evidence that the linearizing assumptions had a basis in fact and were not unreasonable. Second, if the correlation were demonstrable, an attempt could be made to use the theoretical response to predict the transient response of the motor following an imposed program. Thus, if a four forward - four reverse program were imposed, there would be a definite transient oscillating frequency, settling time, etc., as the motor was coming to its steady state condition, following the last four reverse pulses. In theory, for a linear system, if the transient response to a step input is known, then the response to an imposed program should simply be that same response to a step, modified for the effect of initial conditions of position, velocity, etc. If this could be shown to be valid for the stepper motor then its operation as a linear system could be accepted and information

of importance to the design engineer contemplating use of the stepper motor would be readily available. In this manner it would become possible for the design engineer, through use of the defining transfer function, to predict peak overshoot, settling time, etc. for any imposed command group. This concept was not fully realized until after testing was completed and insufficient data was available to justify a general conclusion. It was intended that similar tests be conducted upon both Size 11 and Size 8 step motors (see Illus. 5); unfortunately the Size 8 motor available was a prototype. This motor, upon being commanded to step sequentially, did not respond in equal 90 degree intervals and therefore certain non-linearities were introduced in its transient response.

Linearized Theory for the Stepper Motor

The following assumptions are made before writing the equations governing the response of a step servo motor to a step input (these assumptions will be justified later):

a. the two motor windings which are excited to form a resolved flux vector are mutually perpendicular in every case

b. the resistance and inductance of all windings are equivalent

c. the ampere-turns of each excited stator winding are equal and are zero in the unexcited windings

d. the armature reaction is considered to be zero, i.e. the permanent magnet flux is assumed to be invariant

Due to the discontinuous nature of stepper motor operation a simplified analysis can be attained most easily by viewing the response to a step input voltage; i.e. assume that the winding excitation has been switched to effect a ninety degree rotation but that the rotor is restrained and is not immediately permitted to answer this step input. The effect upon the system is then the creation of initial conditions rather than the imposition of a step input, per se. Then, if e is the angular displacement from the commanded position, i.e. the angular error and if the motor is considered as being formed by two lumped windings which are mutually perpendicular and which are either excited or not excited:

$$T \propto i_1 \cdot \phi + i_2 \cdot \phi \tag{1}$$

where $i_1 \cdot \phi$ represents the dot product of the number one winding "current vector" and the permanent magnet flux vector. When the current in winding two goes to zero the torque may be represented by

$$T = -K \phi i_1 e \tag{2}$$

assuming that torque is a linear function of displacement angle e (or θ), see Fig. 11.

$$T = J\ddot{e} + f\dot{e} \tag{3}$$

$$V_1 = i_1 R_1 + L_1 \, di_1/dt + V_g \tag{4}$$

$$V_g = K_D \frac{d\phi}{de} \frac{de}{dt} = K_g \frac{de}{dt} \tag{5}$$

Equating (2) and (3) and dropping numerical subscripts

$$J\ddot{e} + f\dot{e} = -K \phi i e \tag{6}$$

Substituting (5) into (4)

$$V = i R + L \dot{i} + K_g \dot{e} \qquad (7)$$

$$V = R(i + \dot{i} L/R) + K_g \dot{e}$$

the electrical time constant will be ignored for two reasons

a. in comparison to the mechanical time constant of the system it is negligible; except perhaps as a "dead time" (see Appendix A, Photo. 16 and Chap. VI-1).

b. in this approach the rotor has been considered to be restrained until the electrical transient is completed.

Then, (7) becomes

$$V = i R + K_g \dot{e} \qquad (8)$$

$$i = V/R - K_g \dot{e}/R \qquad (9)$$

Substituting (9) into (6)

$$J \ddot{e} + f \dot{e} = - K \phi e (V/R - K_g \dot{e}/R) \qquad (10)$$

let $K \phi/R = B$

then

$$J \ddot{e} + (f - B K_g e) \dot{e} + B V e = 0 \qquad (11)$$

It can be shown, see Chap. VI-1 and Figs. 8 and 8A, that e (or equally well θ) and the induced EMF are damped sinusoids. Hence, acceptance of the term $B K_g e \dot{e}$ as having negligible effect is justified. Therefore, (11) becomes

$$J \ddot{e} + f \dot{e} + B V e = 0 \qquad (12)$$

where $e(0+) = \pi/2$

taking La Place Transforms and solving for E results in

$$E = \frac{J\,\pi/2\,(S + f/J)}{s^2 + s\,f/J + B\,V/J} \qquad (13)$$

but $\ominus = \pi/2 - E$

therefore

$$\ominus = \pi/2 \left[1 - \frac{J(s + f/J)}{s^2 + s\,f/J + B\,V/J} \right] \qquad (14)$$

The response to a step voltage input of a step servo motor can therefore be approximated by a linear second order expression.

In the actual physical system the rotor responds to the step input voltage and is under no restraint; in order to reflect this the ordinates of Figs. 7 - 10 have been labelled $\ominus_o/V_i$.

2. Motor Failure Response.

In addition to the tests required to determine the transient response of the stepper motor, it was desired to conduct tests which would indicate the operational limits of the motor in responding to a program of forward and reverse pulses. Exhaustive investigation of this parameter included variation of supply voltage and variation of pulse spacing for each program.

It is apparent that at least two factors will effect the motor's ability to answer any given program. First, and presumably foremost, the mechanical inertia of the motor rotor should prevent it from responding with the speed necessary to answer very high rate programs, for the

inertia could be such as to overcome the magnetic forces produced between the flux vector and the rotor. Secondly, and probably much less pronounced, the rotor itself can generate EMF's in the stator windings and thus effectively reduce the strength of the resolved flux vector. Obviously, both of these factors depend to a very great extent upon the speed which the motor rotor attains while attempting to respond to a program. Consequently, it can be presumed that some "worst program" will exist which causes the rotor to attain its highest speed while answering this particular sequence of forward pulses. If such can occur, it is then also possible that, when the pulse program reverses, the inertia of the rotor will cause it to overshoot the last commanded forward position by such an amount that it fails to see some subsequent reverse pulse as one tending to pull it in a CCW direction, but rather as one which pulls it in a CW direction. In the event such a phenomenon does occur, it must be concluded that the stepper motor has failed to follow the command input, and has "lost digital accuracy". The term, "lost digital accuracy" will therefore be used to indicate a malfunction of the stepper motor of such a nature that the motor rotor fails to respond correctly to each pulse of a program, and consequently fails to return to the desired steady state position; synonymously this will be referred to as "motor failure".

Further testing was planned in order to determine the motor's ability to respond to a program of uni-directional pulses, simulating the uni-directional slewing of the motor. In order to view the resolver

envelope on the oscilloscope and obtain meaningful and intelligible data, however, it is necessary to cause the motor to move in such a manner that it has a finite steady state period during which time the resolver envelope is at a null (minimal) value. Then, permanent departures from this steady state null condition during the interval between programs indicate a malfunction of the stepper motor. Consequently, slewing tests consisted of a series of forward pulses followed by a rest time followed, in turn, by a series of reverse pulses which returned the resolver envelope to null. It was anticipated that increasing the pulse repetition rate (PRR) would produce a condition of "synchronous" speed similar to that explained above, which would cause the stepper motor rotor to be unable to settle out to its new commanded position prior to the series of reverse pulses.

VI

TEST RESULTS

1. Transient Analysis.

The results of static torque testing the Size 11 motor are presented on Fig. 6 and, while it is true that little indication of dynamic conditions may be obtained from them, they indicate that initially the torque varies approximately as a linear function of small angular displacements of the rotor.

The transient response of the Size 11 motor to a step input is presented in Fig. 7 as a solid line. The actual response, indicated as the envelope of the 800 cycles per second resolver excitation, was traced from Midwestern Recorder tapes and transferred to a transparency from which a slide was made. This permitted projection of the step response at a suitable magnification level thus allowing response curves to be obtained without the necessity of point by point plotting. In order to facilitate analysis of the step response the curve was magnified approximately twice that presented in Fig. 7; the actual size of the envelope obtained during testing is presented as Rotor Position in Fig. 8. The large projection of the transient response yielded the information listed in Table VI-I.

Assuming 17.3 milliseconds as a resonable half-period of the transient oscillating frequency (see Fig. 7) and using a standard

TABLE VI-I

Step Function
Response Data for a Size 11 Motor

	Normalized Amplitude	Time (milliseconds)
First Peak Overshoot	1.49	21.3
First Peak Undershoot	0.78	38.8
Second Peak Overshoot	1.085	55.5
Second Peak Undershoot	0.97	69.2
First Steady State Crossing	--	13.0
Second Steady State Crossing	--	31.7
Third Steady State Crossing	--	48.9
Fourth Steady State Crossing	--	65.0

approach (Ref. 1, p. 389) the damping factor, ζ, and natural frequency, ω_n, were determined to be 0.27 and 188.1 radians/second, respectively. Using this information the transient response of a second order system was calculated and is presented on Fig. 7 as a broken line. The second order curve is translated three milliseconds to the right in order to compensate for the finite rise time of current in the actual system (see Photo. 16 of Appendix A). Photo. 16 was taken at a sweep speed of one millisecond per centimeter; the scope presentation is ten centimeters in length; and the current rise time is approximately three milliseconds.

It can be said with reasonable certainty that motor size has a direct effect upon this "dead time", i.e. a large rotor inertia will require a significant magnitude of current in the windings before movement occurs and therefore a longer delay time will pass before this magnitude of current is attained. That is, it is physically impossible to impose the step current necessary to produce a step driving force. A comparison of the empirical response with the response of a theoretical second order system shows the correlation to be sufficiently close to permit approximation by second order curves. This justifies the linearizing assumptions made in Chapter V.

In order to demonstrate the value and utility of the step input response information to the designer, the tail-end response of the motor to a four forward - four reverse program was approximated by the theoretical second order curve of Fig. 7 and suitably modified to compensate for the initial conditions being other than zero. Actually, the modification was a factor of unity in this instance and was determined by comparing the respective overshoots in the program response to the overshoots in a linear system responding to a step input. The reasoning, of course, being that if the motor were linear, its response to a step imposed at an instant when there were finite initial conditions (which is the case for the program response) would be changed only by the ratio of the overshoots. It is not suggested that this approach can be used for predicting responses to a program, since to determine the overshoot ratio would require information from the

response to be predicted. The results of this approach do, however, indicate the excellent correlation between the program response and that obtained from a linear second order system (see Fig. 7A). If this is considered sufficient assurance, then the design engineer could take inverse La Place Transforms of the regulating equations, after substituting the initial conditions of interest, and obtain a good approximation of the transient response that could be expected. A possible explanation as to why the overshoot ratio turned out to be unity in this case might be that at the time of imposing the last reverse pulse the potential energy introduced (between instantaneous and commanded rotor position) plus the kinetic energy of the rotor coincidentally equalled the potential energy normally introduced for a step input with zero initial conditions. Other programs that might be checked to verify this theory were not available at the time of this discovery; future investigations in this area could provide decisive information.

Returning to Fig. 7A, the solid line is the transient response of the stepper motor to the last reverse pulse of a four forward - four reverse pulse train; the circled points show the response of a second order system ($\zeta = 0.27, \omega_n = 188.1$). Considering the errors introduced by the magnification process, the approximation is quite good. (The program traces were taken primarily for failure information, therefore that portion of the envelope presently under discussion was of secondary concern at the time of gathering data. Maximum usable recorder amplification was

used for the intermediate part of the failure program, the trailing response therefore being presented at a diminished level. This situation required increased magnification of the trailing response segment of the transient curve thereby increasing the inherent error in the display.)

The imposition of initial conditions appears to have a small but noticeable effect upon the settling time of the Size 11 motor. In the response to a step, the time from first crossover to the time for the response to pass within a $\pm$ 10% tolerance band about steady state is a nominal 47 milliseconds. The response to the last reverse pulse in a four forward - four reverse pulse train damps to within the same band in about 42 milliseconds. It must be emphasized that general conclusions cannot be drawn from this particular case; the results are presented for qualitative purposes only.

Fig. 8 was obtained by analyzing the current information (with load) presented in Fig. 8A; the manner in which this analysis was performed is discussed under Failure Analysis later in this Chapter, where the same basic procedure was used. It is of interest to note the remarkable similarity between no-load currents and the currents obtained when the stepper motor was linked to the resolver through the anti-backlash gear train. The almost complete equivalence of these traces justifies the concept that the pickoff device used (resolver and gear train) had a negligible loading effect upon the motor. Hand loading the motor produced quite square current traces thus indicating the effect of any significant

loading upon the motor, i.e. elimination of the induced EMF humps in the current traces.

Fig. 9 depicts the transient response of the Size 11 motor without anti-backlash gears in the gear train linking the motor to the resolver. (The backlash setup is pictured in Illus. 3.) A gear ratio of 80:1 was used; Photo. 15 indicates the backlash response for a 31.5:1 gear ratio. The degree of backlash introduced by this setup was measured in the following manner: A four forward - four reverse pulse train was imposed and an oscillograph record was made. After the fourth forward pulse, all of the backlash in the system was presumably taken up so when the system was subjected to the first reverse pulse, system backlash became evident. By comparing the different resolver levels a measure of backlash was obtained. For the 80:1 gear ratio used there was found to be 7.9 minutes of backlash in the system. The effect of this backlash is apparent in Fig. 9 but the influence upon digital accuracy is not so obvious. For example, the use of a stepper motor with a 1000:1 reduction gear ratio would result in a resolver rotation of 5.4 minutes for a 90 degree motor rotation. The use of any gear train with magnitudes of backlash amounting to 5.4 minutes or more is out of the question. The necessity of anti-backlash gears when using the stepper motor for all except the crudest of tasks is easily comprehended.

The response of the Size 8 motor to a step input did not lend itself to correlation with a second order system. Initial checks of the Size 8

motor "quadrant accuracy" provided the following information:

Command	Response
0° to 90°	0° to 76°
90° to 180°	76° to 180°
180° to 270°	180° to 256°
270° to 0°	256° to 0°

The importance of the orthogonality of the flux vectors produced by the excited stator coil windings cannot be overemphasized. Physical asymmetry of the coil geometry, non-equivalence of ampere-turns or any other phenomena leading to the production of two flux vectors which are not mutually perpendicular, equal in magnitude and colinear with their conjugates will result in a motor incapable of stepping in precise 90 degree increments. This was the case with the Size 8 motor investigated and the results are clearly demonstrated by the response to a step presented in Fig. 10.

Any one of the anomalies mentioned could produce skewed flux vectors. As the rotor oscillates about its final steady state position in response to a step input it moves not into uniform flux fields on each side of steady state but into fields with greater or lesser strength as a function of the given anomaly. Hence, in moving into a weaker field an overshoot would tend to exceed that for a symmetric system, just as entry into a stronger field would cause a reduction in the magnitude of overshoot (or undershoot). The combined effect is to introduce non-linearity into the response; how

much of this phenomena can be tolerated in a given system can be decided only by the designer.

For these reasons, the transient results for the Size 8 motor and the static torque tests of Fig. 11 are of only qualitative interest.

2. Motor Failure Analysis.

The failure run data indicated in Figs. 12 through 16 were obtained using the Midwestern Recorder tapes of resolver output and current responses in each motor field winding. These data were then analyzed to obtain information on the resolved flux vector and the rotor velocity.

The Midwestern Recorder Oscillograph tapes provided a trace of the modulated 800-cycle envelope representing stepper motor response to an imposed program, and a trace of the current flowing through each stator winding in the stepper motor. The envelope of the resolver output was analyzed to obtain the velocity of the motor rotor by taking finite differences and obtaining approximate average velocities over appropriate time intervals.

As explained in Appendix B, the current traces show the actual current flowing through the stator windings of the stepper motor, therefore, they are a direct indication of the flux being created. Consequently, for analysis, the amplitude of each current was measured at a given time, the U and $\overline{U}$ currents were combined to give a resultant vector and, similarly, the V and $\overline{V}$ currents were combined to give a resultant vector. (Note: the introduction of power gates produced a 180 degree phase

reversal between the motor and the logic circuit.) These two vectors were then plotted on polar coordinates, and a third resolved vector obtained by the vector addition of the resultant vectors. The amplitude and angle of this resolved vector were plotted at the given time.

As an example, refer to Fig. 14, at t = 10 milliseconds the currents are as follows:

U Current = .07

$\overline{U}$ Current = .81 Resultant current = .74 $\overline{U}$

V Current = .71

$\overline{V}$ Current = .21 Resultant current = .50 V

By vector addition on the polar plane, the resolved vector is:

Amplitude = .90 Angle = 56^{o}

Referring to Fig. 13, the resolved flux vector plots show an amplitude of .90 and an angle of 56 degrees at t = 10 milliseconds. Sufficient points were thus obtained to produce a smooth curve of amplitude and angle.

Fig. 15 shows the positions of the motor rotor and the resolved flux vector during steady state and immediately after each individual pulse was imposed. In addition, the direction in which the motor rotor was moving is indicated, as is the direction in which it was being pulled by the flux vector. When following the forward pulse portion of the program, the motor rotor should have been moving continuously in a clockwise direction; and when following the reverse pulse portion of the program, the motor rotor should have been moving continuously in a counterclockwise

direction. (Recall that 360 degrees rotation of the stepper motor rotor results in only 5 degrees rotation of the resolver. Thus, both Figs. 13 and 15 must be used in order to determine whether or not a given program was followed successfully.)

It must be remembered that the flux vector amplitudes shown are not necessarily the correct amplitude in webers. However, the assumption that current was directly proportional to magnetic flux strength is reasonable since good design procedure dictates operation on the linear portion of the B-H curve.

The primary purpose behind showing the resolved flux vector amplitude and angle is to indicate that the induced EMF effect was not sufficient to cause the stepper motor to malfunction. This becomes obvious when Figs. 13 and 15 are analyzed. It can be seen that the stepper motor rotor successfully followed the entire forward pulse train and the first reverse pulse. However, when the second reverse pulse command was given, the stepper motor rotor was almost 220 degrees away from the next commanded position (indicated by the dotted flux vector). Consequently, the rotor answered the pulse, i.e. was attracted to the flux vector, through the lesser 140 degree angle. But this meant that the rotor moved in the forward direction instead of the reverse direction. The third reverse pulse moved the flux vector another 90 degrees counterclockwise. At that time, the angle between the motor rotor and the flux vector was about 300 degrees in the reverse direction, and only 60 degrees in the forward

direction. Therefore, the rotor was again pulled along in the forward direction instead of being moved correctly in the reverse direction. Subsequent pulses caused the flux vector to be rotated counterclockwise until it resumed the steady state position. However, the rotor was moved away from the original steady state position by more than 360 degrees, consequently, when the pulse program ceased, the rotor came to rest at the proper angle, but 360 degrees away from the proper steady state position. Thus, it can be said that the motor lost its ability to reproduce the input, since it did not return to the proper steady state position. Inspection of the flux vector traces on Fig. 13 shows that neither the resolved flux vector nor the resolved flux angle departed appreciably from the values which they assumed when the motor was successfully following a program. The aberrations in flux magnitude and angle were a result of induced EMF and were not sufficient to cause a loss of digital accuracy. Therefore, it can be stated that the failure of the motor rotor was a direct result of mechanical inertia causing the motor rotor to overshoot by such an angle that it was incapable of following the command input. This rotor inertia caused the motor rotor to respond incorrectly to the second reverse pulse of a five forward - five reverse program.

Similar analysis indicates that inertial failures occurred at the second reverse pulse of a three forward - three reverse program and the second reverse pulse of a four forward - four reverse program. Fig. 16 shows the resolver envelope of these programs immediately before and at the time of motor failure.

TABLE VI-II

MOTOR FAILURE DATA FOR SEVERAL PROGRAMS AND SUPPLY VOLTAGES
SIZE 11 MOTOR

Program		Supply Voltage	Pulse Repetition Rate at Motor Failure (pulses per second)
Forward	Reverse		
3	3	-25.5	95
4	4	-25.5	96
5	5	-25.5	101
3	3	-28	96
4	4	-28	98
5	5	-28	106
3	3	-29.5	100
4	4	-29.5	103
5	5	-29.5	107
6	6	-29.5	106
3	3	-31	98
4	4	-31	102
5	5	-31	106
3	3	-33.5	100
4	4	-33.5	106
5	5	-33.5	119

The results of the foregoing tests show that the three forward - three reverse pulse program caused failure to occur at the lowest pulse repetition rate. The average motor failure, with a supply voltage of

-29.5 volts, for the three forward - three reverse program occurred at 100 pulses per second. In addition to this failure testing at -29.5 volts, failure runs were conducted at -25.5, -28, -31, and -33.5 volts supply voltage. From Table VI-II it is apparent that the pulse repetition rate at motor failure varied with the supply voltage. However, it should be noted that the three forward - three reverse program was the worst in every instance.

Further investigations were conducted to ascertain the effect of applying a sequence of pulses in one direction, (slewing response) followed by a finite rest time, and then applying an oppositely directed sequence of pulses in order to return the resolver to the null position. The Wang Pulse Generator could only provide a combined total of 12 forward and/or reverse pulses although the word length could be made 64 digits long. Thus, the two practical programs available were the four-four-four and three-six-three. Table VI-III shows the results of these tests. It is clear that the performance of the motor was greatly

TABLE VI-III

MOTOR FAILURE DATA FOR PROGRAMS WITH FINITE REST TIME
SIZE 11 MOTOR

Program				
Forward Pulses	Rest Time	Reverse Pulses	Supply Voltage	Pulse Repetition Rate at Motor Failure (pulses per second)
3	6	3	-29.5	175
4	4	4	-29.5	172

improved by providing a finite rest time between the forward pulse sequence and the reverse pulse sequence.

In order to determine what effect, if any, would result from instantaneous imposition of a program of pulses at a relatively high pulse repetition rate, the drive circuit input was disabled and then enabled while the Wang Pulse Generator was pulsing at a rate just slightly less than the motor failure rate shown in Table VI-II. In every case, the motor responded correctly. Failure could only be caused by increasing the pulse repetition to the value shown in Table VI-II. Therefore, it seems reasonable to assume that stepper motor failure in response to a program of pulses was independent of:

a. method of imposing program, and

b. pulse width,

and, that stepper motor failure was a definite function of:

a. number of forward and reverse pulses applied

b. pulse repetition rate

c. stepper motor stator coil supply voltage

d. rest time allowed between forward pulse train and reverse pulse train.

Of course, the foregoing is true only if the geometrical, ampere-turn and other requirements mentioned under Transient Analysis are met.

Finally, in order to obtain a general pattern of motor behavior for increased pulse repetition rate from well below the failure PRR to well

above the failure PRR, a three forward - three reverse program was imposed and pulse spacing decreased while motor behavior was observed qualitatively. The motor behavior was as follows:

a. Motor followed normally.

b. Motor began to miss pulses (the failure point).

c. Motor began to run continuously in one direction.

d. Motor ceased running continuously and began to oscillate rapidly (pulse repetition rate approximately equal to 200 pulses per second).

e. Motor began to run continuously again, but at a much slower RPM than in c. above. (This occurred at a PRR equal to 290 pulses per second; the same PRR at which logic circuit failure occurred - see Appendix B.)

f. Motor ceased running continuously and began to oscillate at a frequency even higher than that in d. above. (PRR was approximately 625 pulses per second and logic circuit was dividing.)

g. Motor began to run continuously in one direction. (Logic circuit response indicated that the logic circuit was answering only one input pulse, and thus was sending only one step to the motor.)

It is obvious that true motor response ended at b. above. However, when properly excited by the logic circuit, the motor was capable of extremely high speed, very-small-amplitude oscillations.

Size 8 - Analysis of Failure Run

Fig. 17 shows the resolver envelopes for the Size 8 stepper motor just before and at failure in response to a five forward - five reverse program.

Several interesting features are apparent in Fig. 17. First, both the upper and lower traces show motor failure due to a five - five program. The upper trace is the response which resulted when the motor rotor was at an initial position of 329 degrees; this corresponded to a logic circuit condition of U and V energized (this was really the condition on the motor side of the power gate). The lower trace is the response which resulted when the motor rotor was at 149 degrees in the steady state; this corresponded to a logic circuit condition of $\overline{U}$ and $\overline{V}$ energized (again on the motor side of the power gates). In the first instance, motor failure occurred when the pulse spacing was decreased to about 8.5 milliseconds. However, when the motor rotor was at an initial position of 149 degrees, failure did not occur until pulse spacing was reduced to 5.8 milliseconds. The failure at a pulse spacing of 8.5 milliseconds will hereafter be referred to as the "anomalous" failure and the failure at 5.8 milliseconds as the normal failure,.since, for a three forward - three reverse program failure occurred at a spacing of 7.6 milliseconds and for a four forward - four reverse program at a spacing of 6.4 milliseconds; therefore, it is reasonable that spacing at failure should decrease below 6.4 milliseconds for a five forward - five reverse program,

and the assignment of the 5.8 milliseconds spacing as a normal failure would appear to be plausible.

Recalling that the Size 8 motor has a marked asymmetry in its windings; the motor rotor positions were:

IDEAL (in degrees)		ACTUAL (in degrees)		DEGREES OF ROTATION	
From	To	From	To	Ideal	Actual
315	45	329	45	90	76
45	135	45	149	90	104
135	225	149	225	90	76
225	315	225	329	90	104

It is seen that failures occurred when the motor rotor was within the 104 degree arc. Further analysis has shown that the behavior of the resolved flux vector was essentially the same for both the normal and anomalous failures. Consequently, it must be presumed that this failure was peculiar to the particular motor tested and was, perhaps, a result of unmeasured aberrations in the flux field, pole spacing and winding geometries.

The relative effects of reducing motor size are, however, portrayed in the transient response (see Fig. 10) as well as the failure runs in Fig. 17. The transient oscillating frequency was apparently increased and the "dead time" effects due to motor winding time constant were reduced. Reluctance path considerations were not investigated in any

detail but it should be mentioned that the Size 8 motor was influenced visibly by this phenomenon significantly more than the Size 11 in any case. Hand rotation of the motor shaft was met with little opposition in the Size 11; in rotating the shaft of the Size 8, however, a definite "rachet effect" could be felt as the permanent magnet rotor passed by the stator slots and exhibited a pronounced preference for remaining in the path of least reluctance. In order to maximize the torque producing capabilities of the smaller motor the air gap between rotor and pole pieces was apparently reduced in a greater proportion than the decrease in motor casing size. If this design philosophy is always followed it may be presumed that magnetic path effects may play a larger role in both the transient response and the failure point of the Size 8 motor.

VII

CONCLUSIONS

On the basis of the results of the preceding investigations, it can be concluded that small step servo motors are very useful as pulse integrators in both control and computer applications. Their shaft output can be used to produce the algebraic sum of an input consisting of discrete pulses.

Specifically, it was determined that the Size 11 Stepper Motor transient response to a step input could be approximated using linear second order theory. Application of this theory to determine the damping ratio, natural frequency, transient oscillating frequency, and settling time, required that certain linearizing assumptions be made. The actual damping ratio and natural frequency obtained by testing the Size 11 Motor were $\zeta = 0.27$ and $\omega_n = 188.1$ radians/second.

Experimental results implied that response to a program could be predicted from linear second order theory but insufficient data were available to justify a general statement. The derivation of a generalized theory for the stepper motor requires consideration of reluctance path effects upon motor response.

In addition, it was shown that the Size 11 Stepper Motor was limited in its ability to respond to a program of sequential pulses. This limitation was a result of rotor inertia overcoming the magnetic attraction between the resolved flux vector and the permanent magnet rotor. Thus,

the effect of rotor size upon the point at which digital accuracy is lost must be weighed against the torques which the motor will be required to produce and a design compromise made.

It was also demonstrated that there existed a "worst program" of sequenced pulses; this program caused the motor rotor inertia to induce motor failure at a lower pulse repetition rate than any other program. For the Size 11 Motor, the worst program was one of three forward pulses followed immediately by three reverse pulses; with loss of digital accuracy occurring at approximately 100 pulses per second.

REFERENCES

1. Truxal, J. G., Automatic Feedback Control System Synthesis, McGraw-Hill Book Co., Inc., New York, 1955.

BIBLIOGRAPHY

Ahrendt, W. R., Servomechanism Practice, McGraw-Hill Book Co., Inc., New York, 1954.

Chestnut, H. and R. W. Mayer, Servomechanisms and Regulating System Design, Vol. II, John Wiley & Sons, Inc., New York, 1955.

Fitzgerald, A. E. and C. Kingsley, Jr., Electric Machinery, McGraw-Hill Book Co., Inc., New York, 1952.

Thaler, G. J., Elements of Servomechanism Theory, McGraw-Hill Book Co., Inc., New York, 1955.

"Step Servo is Natural Mate for Digital Computer", Military Systems Design, pp. 128-129, May-June, 1959.

APPENDIX A

OSCILLOSCOPE PHOTOGRAPHS

This Appendix is composed solely of oscilloscope photographs of the responses of the logic circuit or stepper motor. It is intended to provide a qualitative indication of circuit or motor performance and should not be used to obtain quantitative information. All the photos contained herein were made with a Land Polaroid Fixed Focus Camera mounted on the face of a four-gun oscilloscope. Since the Land Fixed Focus Camera was designed for use with conventional circular tube cathode-ray oscilloscopes, it was not possible to completely compensate for the square face of the four-gun scope. Consequently, the image sharpness of these photos is not quite up to standard. Nonetheless, they provide a qualitative representation of circuit and motor response.

APPENDIX B

EXPLANATION OF LOGIC CIRCUIT MODIFICATIONS

1. RC Coupler Modification

Initial attempts to determine stepper motor limitations met with no success, for, in every instance, the logic circuit state moved one step forward immediately prior to what appeared to be motor failure. There was no immediately obvious reason for logic circuit failure. Therefore, in order to investigate thoroughly the logic circuit response, it was disconnected from the stepper motor and 150-ohm resistors were substituted for each motor stator winding (since the measured resistance of the coils was 150 ohms $\pm$ 5 ohms). Then the Wang Pulse Generator output was fed, through the emitter-follower, into the logic circuit, and the logic circuit output, across the 150-ohm resistors, was measured. Thus, the voltage waveforms across the simulated windings could be viewed on the oscilloscope.

Photos. 1 through 6 of Appendix A show logic circuit responses to various programs. Photo. 1 shows the response immediately prior to circuit failure for the one forward pulse program (upper section) and the one forward followed by one reverse program (lower section). Photos. 2 through 6 indicate the response of the logic circuit to two forward - two reverse, three forward - three reverse, four forward - four reverse, five forward - five reverse, and six forward - six reverse programs. Each of these photographs shows the logic circuit response immediately prior to

and immediately after logic circuit division occurred. For example, in Photo. 3, the upper oscilloscope photograph shows the logic circuit responding properly to all forward and reverse pulses; in the lower photograph, however, it is seen that the logic circuit fails to answer the first reverse pulse. Similarly, all other lower photographs of this set show the logic circuit failing to answer the first reverse pulse.

With a forward pulse train applied, the logic circuit ceased to respond (by normal flipflop action) and began dividing (answering every other pulse) at a pulse repetition rate of 155 pulses per second. Next, a program of one forward pulse immediately followed by one reverse pulse was applied to the logic circuit. The logic circuit responded correctly, only one flipflop operating, until a pulse repetition rate of 80 pulses per second was attained, at which time both flipflops were activated by the input, and division occurred. Oscilloscope investigation of the waveforms at nodes within the logic circuit indicated that the time constant of the RC coupler immediately preceding the steering diode was so high, RC = 7.5 milliseconds, that it could not recover in the 6.5 milliseconds between pulses of the one forward pulse program.

Since a forward pulse followed by a reverse pulse should trigger the same flipflop, it then became obvious that the logic circuit failure was a result of the inability of the RC coupler to pass the two consecutive pulses. Consequently, the time constant of this coupler was changed to 2.2 milliseconds by substituting a 22 kilohm resistor and a 0.1 microfarad capacitor.

TABLE B-I

LOGIC CIRCUIT LIMIT TEST RESULTS
(with 150-ohm resistors simulating motor windings)

Program	Word Length (bits)	PRR at Failure (pps)	Remarks
1 fwd.	21	560	
1 fwd. - 1 rev.	21	288	
2 fwd. - 2 rev.	21	286	
3 fwd. - 3 rev.	21	286	In all cases logic circuit began dividing.
4 fwd. - 4 rev.	21	290	
5 fwd. - 5 rev.	21	295	
6 fwd. - 6 rev.	21	275	

Table B-I shows the pulse repetition rate at failure for the various programs imposed with the 150-ohm resistors simulating the windings. From Table B-I it is apparent that, with this new coupler, the logic circuit limitation for a uni-directional program was about 1.8 milliseconds pulse spacing (PRR = 560 pps) and for all bi-directional programs was about 3.5 milliseconds (PRR = 288 pps). These tests were conducted on both channels of the logic card, and results were almost identical.

2. Power Gate Modification

Having reduced the time constant of the steering diode RC coupler to an acceptable value, the logic circuit was reconnected to the motor windings and runs were made to determine the pattern of motor response

during normal operation. Photos. 7 through 10 show typical resolver output envelopes for various input programs. It is clear that the stepper motor was following the command faithfully. Then, pulse spacing was reduced to investigate the time of motor failure. However, as pulse spacing decreased, the flipflop voltage traces began to lose their square wave characteristics. These departures resulted from EMF's generated in the windings of the motor. Photo. 11 (upper photograph) shows a voltage trace with these pronounced induced EMF effects.

As the pulse repetition rate was increased, it became obvious that the logic state at some point within the program would change. Photo. 11 shows the $\overline{U}$ voltage; in the upper section can be seen the voltage at a high pulse repetition rate, with its pronounced induced EMF "hump"; in the lower section is seen the same $\overline{U}$ voltage with the pulse repetition increased by a very slight amount, and it is apparent that the region where the previous EMF "hump" was has now changed state to $\overline{U}$ energized. (The "base line" for the traces is approximately -27 volts, and this condition exists when a coil is not energized; i.e. when the associated transistor is cut off. A change to the energized condition is indicated by the rise of the trace from -27 volts to approximately -4 volts.) These phenomena occurred at relatively low pulse repetition rates (76 pulses per second in Photo. 11), and thus prevented analysis of the failure point of the stepper motor.

Concurrently with the check of response to reduced pulse spacing for various programs, a program of checking the effect of varying $\bar{B}$

TABLE B-II

VARIATION OF LOGIC CIRCUIT FAILURE WITH SUPPLY VOLTAGE WHERE FAILURE IS A RESULT OF INDUCED EMF EFFECT

Pulse Program		Supply Voltage	PRR At Logic Circuit Failure (pps)	Remarks
Forward	Reverse			
3	3	-22	60	
4	4	-22	61.5	
5	5	-22	58	Worst Program
6	6	-22	60.5	
3	3	-24	64	
4	4	-24	70	
5	5	-24	60.5	Worst Program
6	6	-24	64.5	
3	3	-28	71	
4	4	-28	75	
5	5	-28	66	Worst Program
6	6	-28	(no data)	
3	3	-29.5	72	
4	4	-29.5	82	
5	5	-29.5	69	Worst Program
6	6	-29.5	77	

Note: All above data based upon a steady state flipflop condition of $\overline{U}$ and $\overline{V}$ energized. Data for U and V energized is identical. To obtain data for $\overline{U}$ and V energized or U and $\overline{V}$ energized, decrease each of above readings approximately as follows:

3 forward - 3 reverse : 25%
4 forward - 4 reverse : 15%
5 forward - 5 reverse : 13%
6 forward - 6 reverse : 9%

(stator) supply voltage was in progress. Table B-II shows the results of these voltage variation tests. In essence, the ability of the motor to respond to various programs is directly related to the motor stator supply voltage. As voltage decreases, the limiting pulse repetition rate decreases for each type of program. It should be noted that the lowest pulse repetition rate limit was obtained using a five forward - five reverse pulse program with -22 volts to the stator windings.

As explained below, these failures were caused by induced EMF's. The motor rotor attained its greatest angular velocity when the five forward - five reverse pulse program was applied; therefore, the induced EMF was greatest for that program. It would seem that the six forward - six reverse program should have caused equal or greater rotor velocity but some reflection on the command sequence will indicate why it did not. The sixth command could have rotated the resolved flux vector to such a position, relative to the instantaneous location of the rotor that a retarding force was exerted. Consequently, a smaller induced EMF was generated. Thus, because of its larger induced EMF's, the five forward - five reverse program caused earliest failure.

The logical explanation for this phenomena is to be found in the analysis of the effects of the EMF generated by the stepper motor. (See Fig. 1). By viewing the signal at the common emitter junction, it was possible to verify the fact that the induced EMF produced a sufficiently strong signal to falsely trigger the flipflops. Consider,

then, Fig. 1 with Q1 of the U flipflop in a saturated condition: then the S2-S3 motor winding is conducting heavily. It was established experimentally that the induced EMF in the motor winding can attain a nominal value of some 10 volts; this means that an effective - 19 volts appears at S3 (since the entire voltage drop must be -29 volts, and 10 volts of this was being supplied by induced EMF, the resultant is -29 + 10 = -19), but the S3 side of the $\overline{U}$ line is known to be at about -4 volts, so -15 volts is being dropped across the internal resistance of the motor winding instead of -25 volts. This means that less current is being drawn in this winding. But, if less current is being drawn, then less emitter current is flowing. Less current running in the emitter leg means a smaller voltage drop across the 32-ohm resistor (at the common emitter), i.e. instead of being at -4 volts, this voltage level will be nearer ground. This will tend to send Q2 into conduction, cutting off Q1 due to cross-coupling action. The U flipflop then changes state, and the logic circuit "fails" on a false impulse resulting from the induced EMF. (For an explanation of circuit operation see Appendix C.)

During the foregoing tests, a definite pattern of circuit failure became apparent. Failure points seemed to be dependent upon the steady state condition of the logic circuit flipflops (the initial angular position of the resolved flux vector). In fact, it was noted that there was a definite relation between the failure points and the initial angular location of the resolved flux vector. When either U and V or $\overline{U}$ and $\overline{V}$

were energized, failure occurred at a somewhat higher pulse repetition rate than when $\overline{U}$ and V or U and $\overline{V}$ were energized. This phenomenon was repeatable for all values of supply voltage. In every case, the failure was a logic circuit failure due to induced EMF's reflected back into the drive circuit and not a motor failure, per se.

The explanation for the difference in failure points as a function of resolved flux vector initial position is relatively simple. Consider Fig. 2; it will be noted that the resolved flux vector will rotate 180 degrees when the logic state changes from U and V energized to $\overline{U}$ and $\overline{V}$ energized; similar rotation occurs when the logic state changes from $\overline{U}$ and V energized to U and $\overline{V}$ energized. Very slight variations in logic circuit component values and motor winding inductances and resistances can cause the strengths of these resolved flux vectors to be different, particularly under dynamic conditions. However, the resolved flux vectors seem to occur in pairs: a U-V and $\overline{U}$-$\overline{V}$ pair and a $\overline{U}$-V and U-$\overline{V}$ pair. The vectors in each pair were not conjugates, and the pairs were not of equal magnitude nor mutually perpendicular. Thus, the strength of the resolved flux vector will be a function of the initial position of the flux vector and since the torque exerted on the rotor is, in turn, a function of flux strength, variations in these starting torques are to be expected. Greater torques will cause the rotor to move more rapidly, and, since induced EMF is proportional to $\frac{d\theta}{dt}$, such induced EMF will be larger. This larger induced EMF will cause the voltage variation effects previously detailed to occur earlier, and thus

cause logic circuit failure to occur earlier. However, it must be emphasized that these variations are small and may not be susceptible to elimination by engineering design, since they are a result of normally acceptable variations in components.

In order to prevent this false triggering of the logic circuit, a power gate buffer stage was added to the test circuitry. This additional circuit, which was nothing more than a set of transistorized relays, is shown schematically in Fig. 3. The action of the power gate circuit in eliminating the induced EMF effect in the logic circuit is plain in Photo. 12, which shows the $\overline{U}$ and $\overline{V}$ voltages on the logic circuit side of the power gate buffer. The introduction of the power gate circuit permitted conclusive testing of the stepper motor response independent of power flipflop deficiencies.

A more pronounced and clearer indication of the effect of the induced EMF's in the motor windings themselves is shown by the "current traces" of Photos. 18 through 21. These photographs show the voltage across a 3.3 ohm resistor in series with each of the motor windings, and therefore may be regarded as current traces. The photographs were taken when pulse spacing was 10.1 milliseconds; just shortly prior to stepper motor failure. This technique for obtaining winding currents was repeated during motor failure testing with power gates using 10 ohm resistors in series with the windings (see Chapter VI).

APPENDIX C

DETAILED EXPLANATION OF LOGIC CIRCUIT OPERATION

A simplified explanation of logic circuit operation is contained in Chapter III. The following is a detailed discussion of the manner in which the logic circuit is designed to cause sequential excitation of motor stator windings and corresponding rotation of the resolved flux vector.

1. "And" and "Or" Gate Operation.

Referring to Fig. 1, the "forward in" (F) and "reverse in" (R) pulses entering the circuitry are negative type pulses. Their polarity is reversed by 2:1 step-up transformers (dotted side of winding to RF ground, hence the pulse is inverted). The "and" gate is formed by three diodes. One of these in each case (F or R) is held at -12 volts. The U, V, $\overline{U}$, $\overline{V}$ diodes are either at -4 or -27 volts depending on the state of the U and V flipflops. Consider as an isolated example the FUV "and" gate. The "and" gate operates such that the most negative voltage present at the cathode of one of the three diodes (FUV) becomes the voltage of the plate node, i.e. the plate is clamped (lossless diode) to the most negative potential present on the cathodes of the diodes. Thus, if either U or V are at -27 volts, a positive pulse into F will not be passed by the "and" gate since the plate node of FUV is at -27 volts. If, however, U and V are both at -4 volts, then the F diode is in a commanding position, i.e. with the plates of the F, U and V diodes at -12 (because F is at -12),

if a positive pulse is placed on the cathode of the F diode it will be passed. This positive pulse on the F cathode has the form

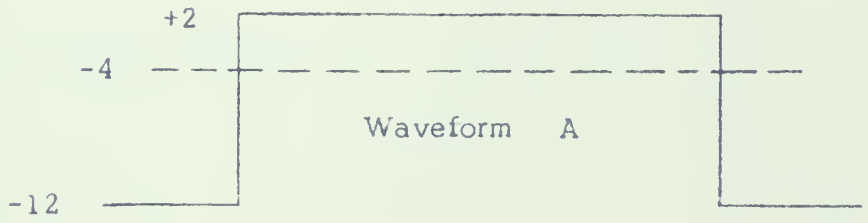

As the cathode of the F diode rises from -12 volts, the plate node(s) will follow this rise in slave fashion until the F cathode rises above -4 volts at which time the F diode is cut off. Thus, the net effect is for the "and" gate to pass a positive pulse of the form

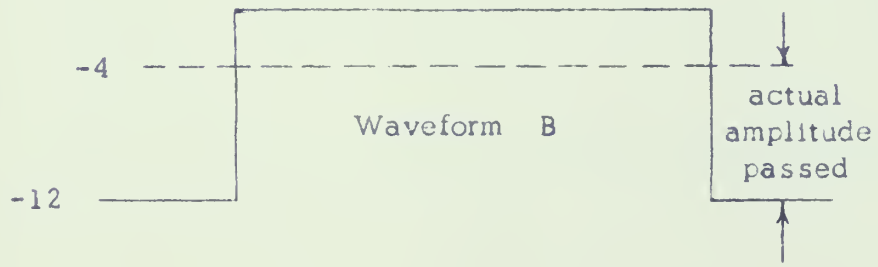

This is directly coupled to the "or" gate. The "or" gate operates such that the cathode nodes of the "or" gate diodes assume the most positive potential of the four available. Since the cathodes of the "or" gate diodes are all held at -12 volts, as soon as the plate of any "or" gate diode begins to rise above -12 volts that diode will conduct. Hence, in the case of the FUV "and" gate passing the B waveform, the topmost diode of the Q3 "or" gate in Fig. 1 will conduct and faithfully pass the

B waveform. The transistor Q3 is arranged to pass a positive pulse imposed upon the base of Q3; thus Q3 operates as an "emitter-follower driver".

2. Operation of the Binary Flipflop Circuit.

The circuitry is designed such that one collector voltage is -27 volts when the other is -4 volts, see Fig. 1. Assume the collector of Q2 is at -27 volts (since the power supply is -29.5 and each motor winding is approximately 150 ohms causing a nominal 2.5 volt drop). The right plate of the coupling capacitor to Q2 is therefore at -27 volts and the left plate is at -12 before any signal is imposed. Since the collector of Q1 is at -4 the base of Q2 is at about -1.5 due to the 2 kilohm - 1 kilohm voltage divider. Under these conditions, the Q2 steering diode is in a non-conducting condition.

It would appear that similar circumstances would dictate a -9 volt potential on the base of Q1. The power transistor, however, operates such that the collector and emitter are approximately at the same voltage levels; in this case -4. The emitter-base junction of Q1 then acts as a conducting diode and a heavy current flow occurs from emitter to base, this causes a very heavy collector current and the Q1 transistor is in its saturation state. The -4 potential is the clamping level sought since the emitter resistance is only 32 ohms and this low impedance will govern the clamping level. The 22K resistor plays no role during the saturation condition but enters the picture in the cutoff mode by arranging for the

steering diode of the cutoff transistor to be non-conducting.

The Q1 steering diode is in a conducting condition, or at least ready to conduct. When the "positive" pulse comes in from the emitter-follower it is insufficient to drive the Q2 steering diode into conduction and is passed to the base of the Q1 transistor which is cut off by the pulse. The Q1 collector heads toward a -27 volt potential and the drop is coupled to the Q2 base driving it into conduction.

The same conditions now pertain as before, but for the opposite transistor. The binary circuit has thus experienced a change of state. This change must be supplied to the logic matrix in order that it be in the correct condition to properly direct any succeeding pulses to the correct flipflop. This intelligence must not be transmitted so quickly, however, that the "and" gates assume their new condition before the incoming pulse has had sufficient time to decay, i.e. the prospect of false triggering of the new matrix condition with the tail end of the same pulse which began the sequence must be avoided. To accomplish this, the intelligence is delayed by a typical RC delay circuit. The final voltages indicating the state of the flipflops to the "and" gates is reached well after the incoming pulse; i.e. after the incoming pulse has decayed to an amplitude incapable of producing a false trigger. Meanwhile, of course, the stepper motor rotor moves along to the orientation dictated by the new resolved magnetic flux vector.

The two 6766 Hughes diodes are used for damping purposes, to prevent surges in the motor windings.

APPENDIX D

NAMEPLATE DATA OF TEST EQUIPMENT

Audio Signal Generator, Model 205AG, Hewlett-Packard Company

Cathode Ray Oscilloscope, Four-Gun, Model K-470, Electronic Tube Corporation

EPUT Meter, Model 5210R-1, Beckman Instruments Company

Oscillograph, 18 Channel, Model 616, Midwestern Instruments, Inc.

Oscilloscope, Twin Beam, Type 531, with Type CA Dual Trace Plug-In Unit, Tecktronix, Inc.

Programmed Pulse Generator, Model 612A, Wang Laboratories, Inc.

Pulse Motor, Model P022P SM 8, American Electronics, Inc.

Regulated Power Supply, 0 - 18 volts, 1 ampere, Model SC-18-1, KepCo Laboratories

Regulated Power Supply, 0 - 36 volts, 1 ampere, Model SC-36-1, KepCo Laboratories

Resolver, Part No. R-211, Luther Manufacturing Company

Resolver, Differential, Type 3R982-013, Kearfott Company, Inc.

Resolver, Synchro, Model IR11N8-155, American Electronics, Inc.

Step Servo Motor, Part No. 9711-050, Induction Motors of California (two used)

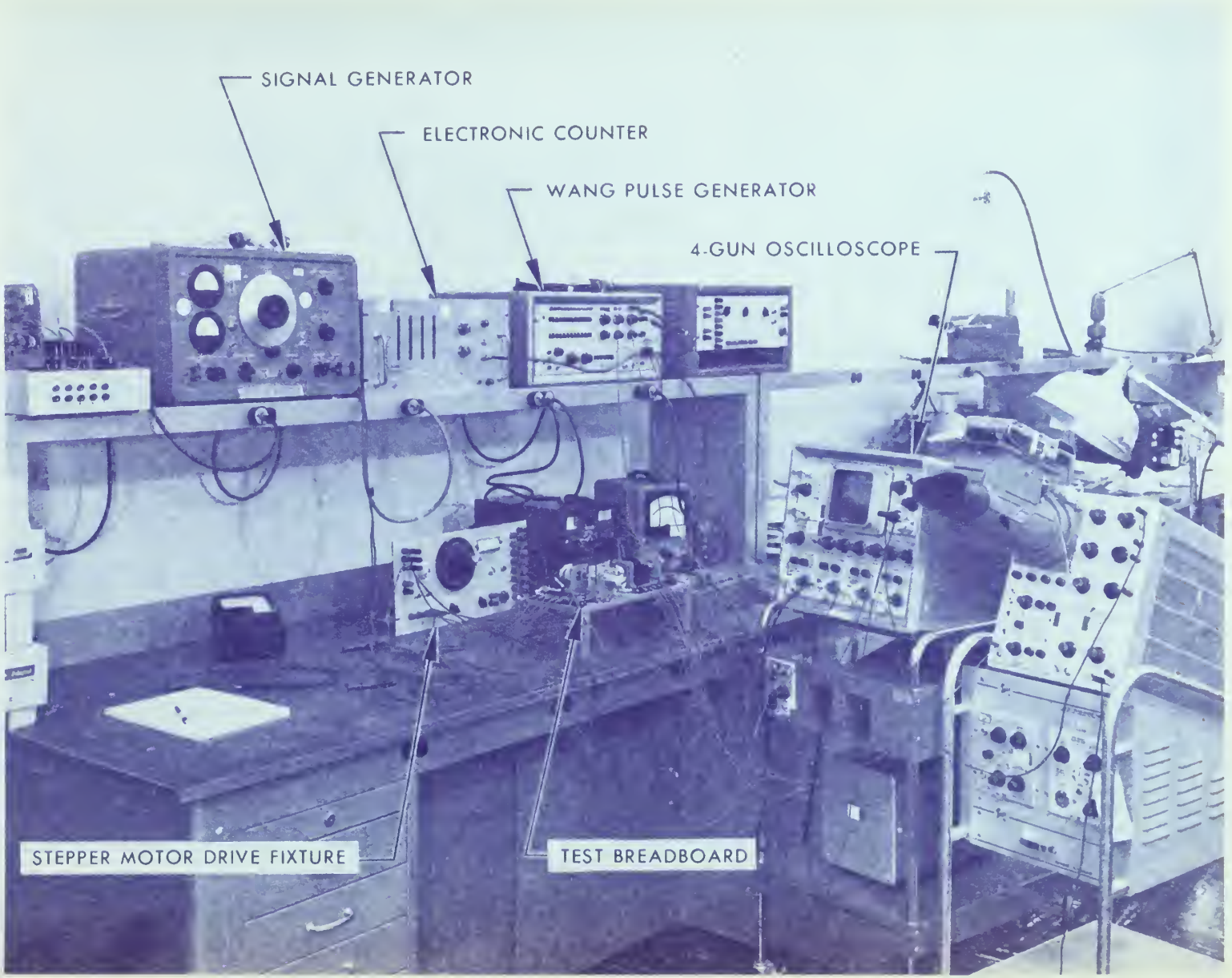

Illus. 2 General Arrangement of Stepper Motor Test Equipment and Testing Area

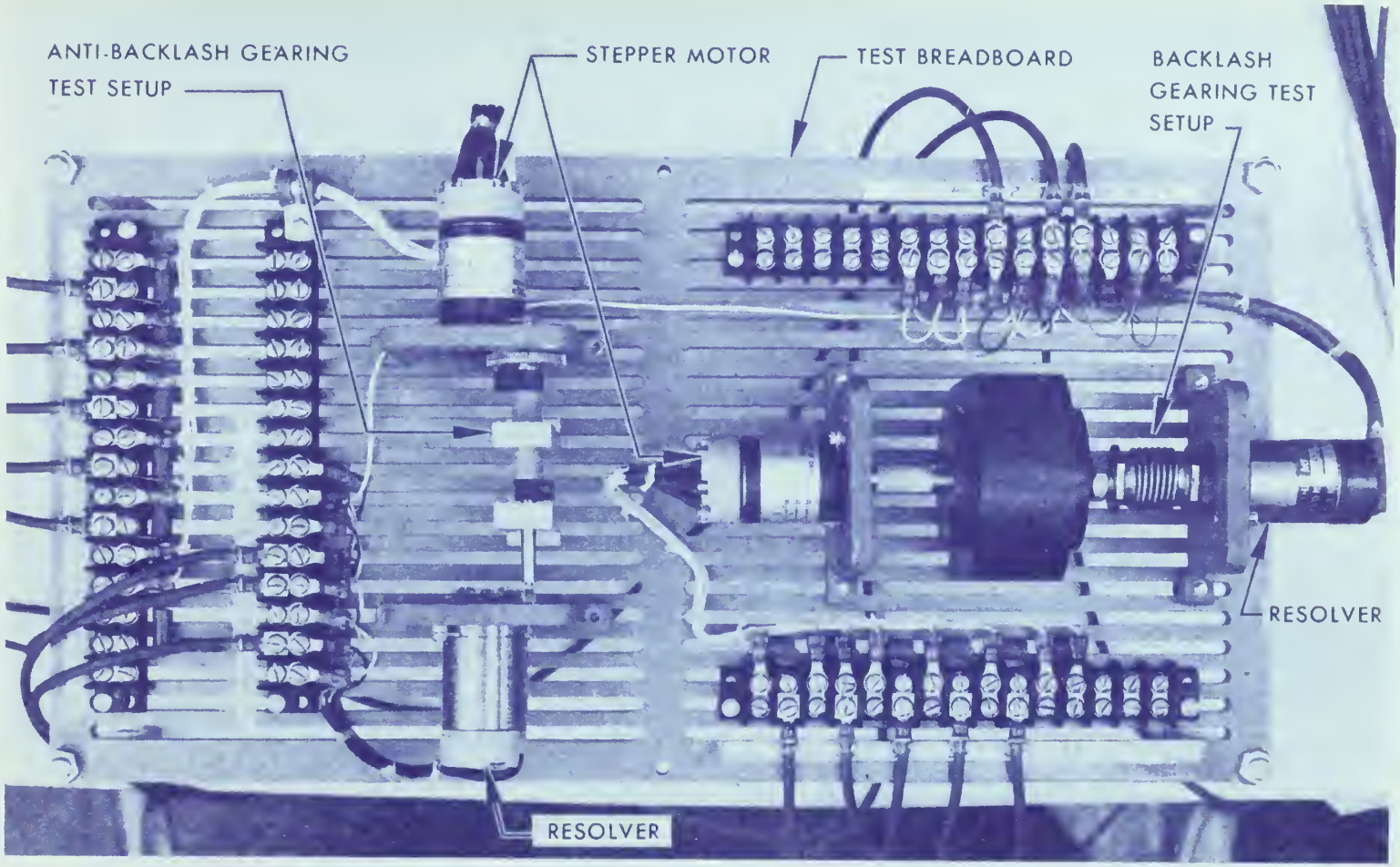

Illus. 3 Test Breadboard No. 1 Showing Gear Trains with and without Anti-Backlash Gearing

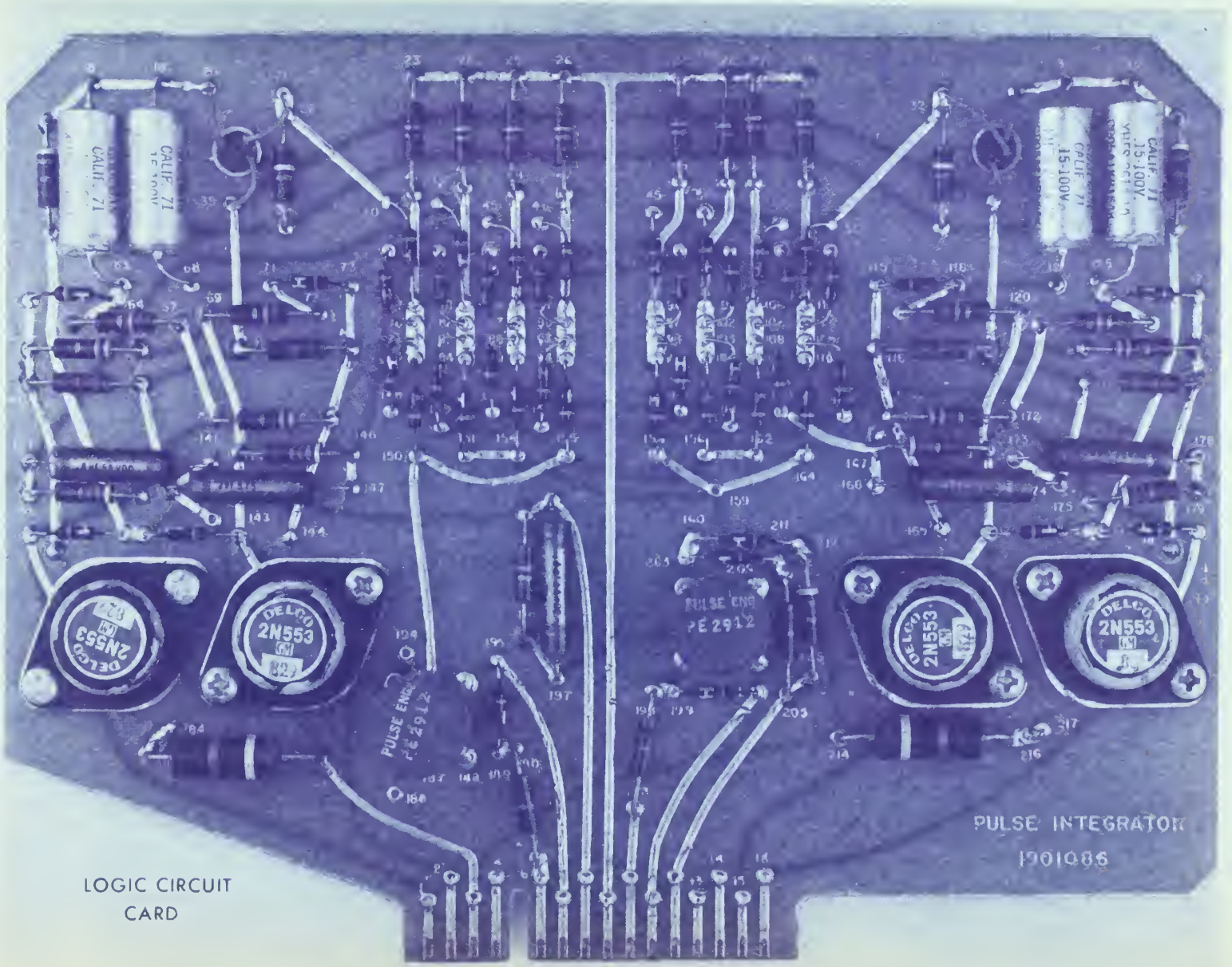

Illus. 4 Logic Circuit Card

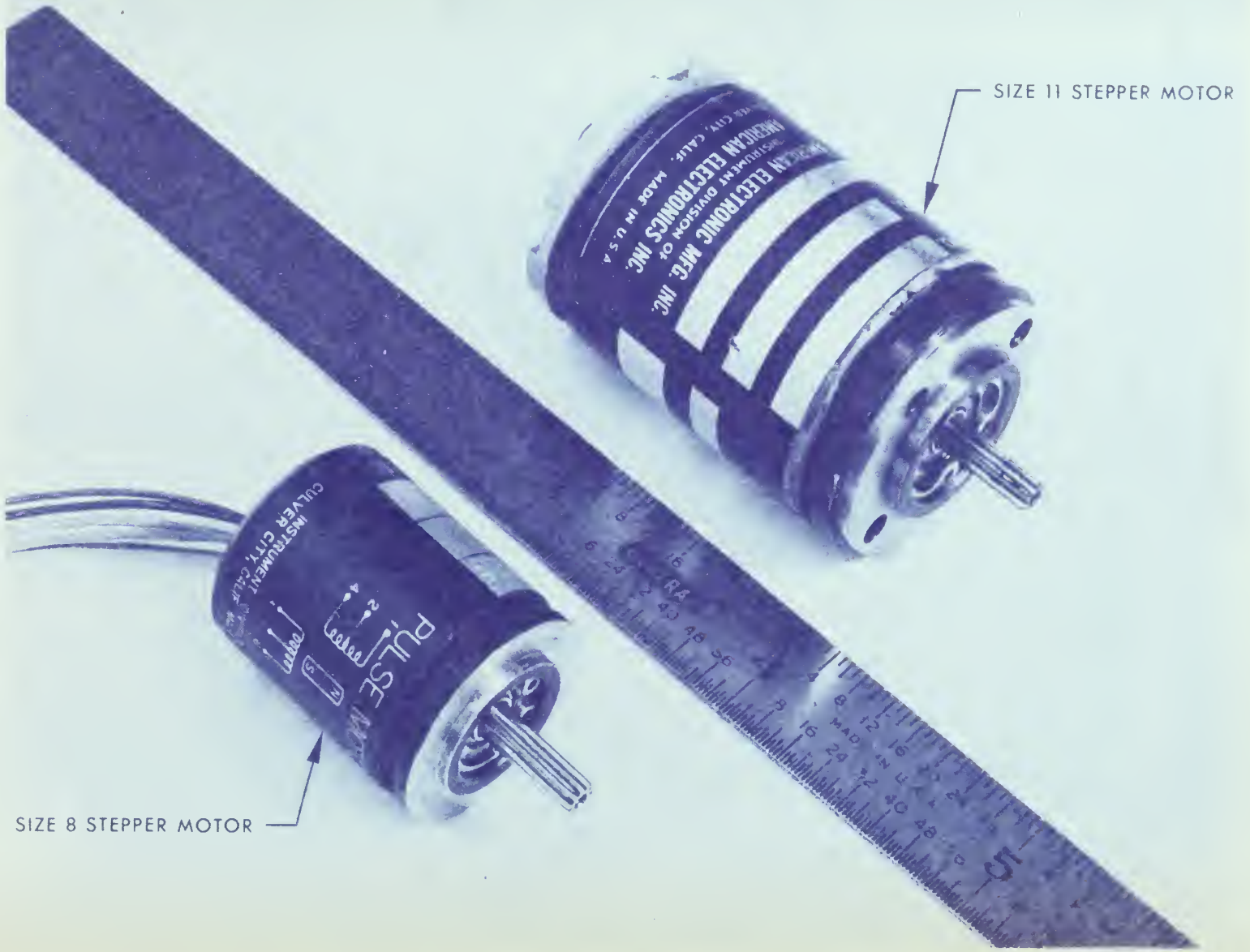

Illus. 5 Comparison of Size 11 and Size 8 Stepper Motors

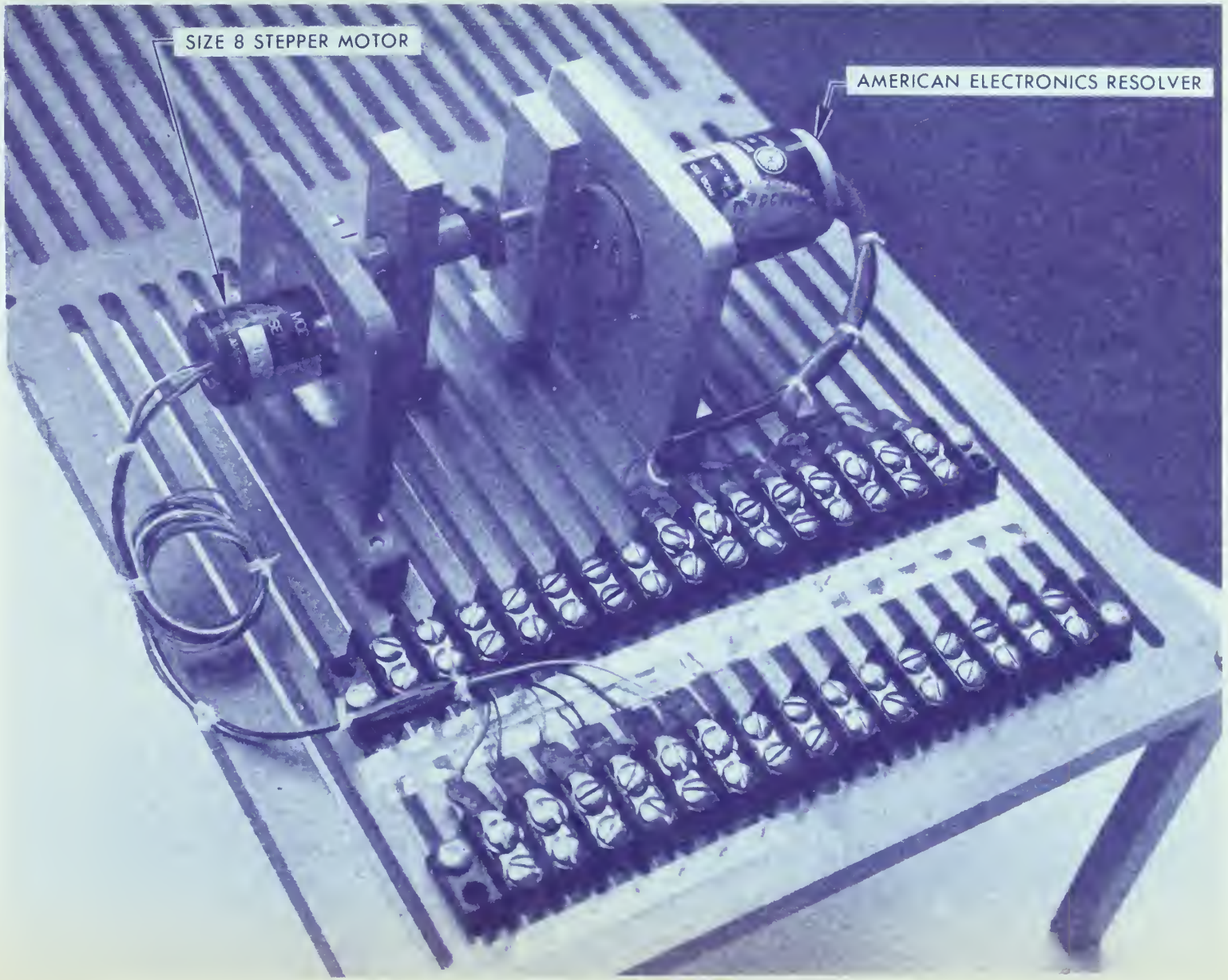

Illus. 6 Test Breadboard No. 2 Showing Anti-Backlash Gearing with Size 8 Stepper Motor

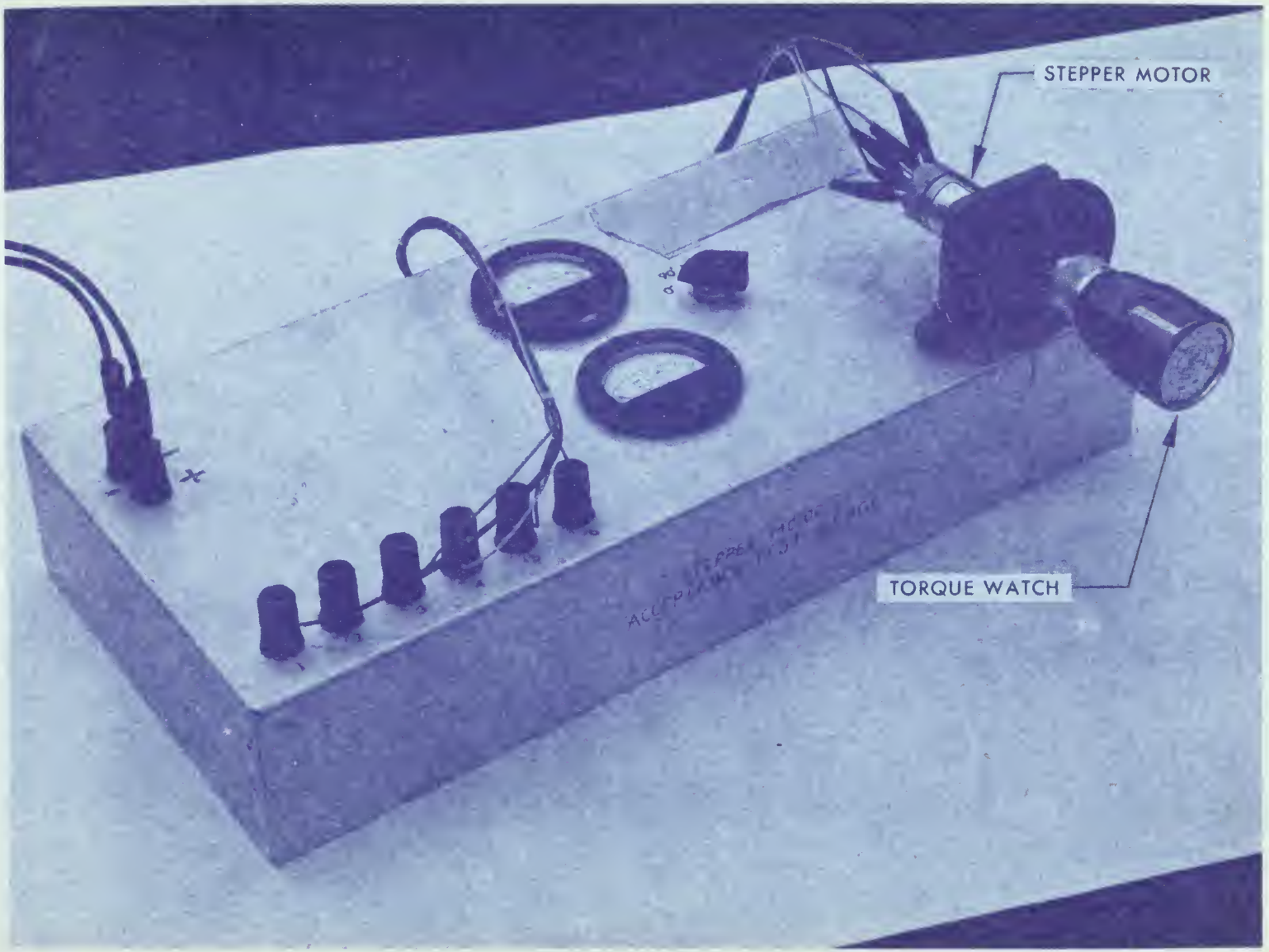

Illus. 7 Stepper Motor Acceptance Test Kluge for Static Torque Testing

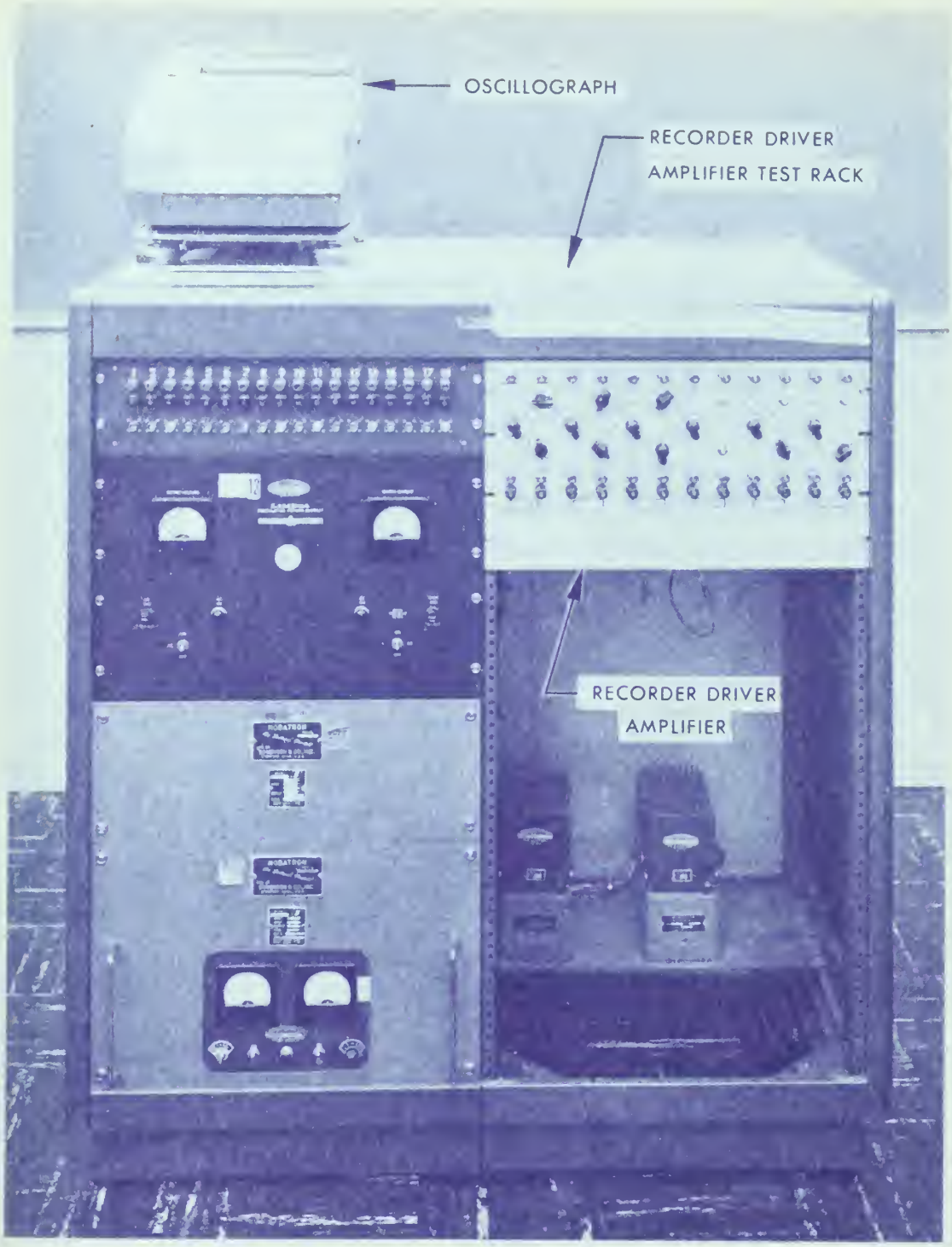

Illus. 8 General View of Midwestern Recorder and Amplifier Chassis

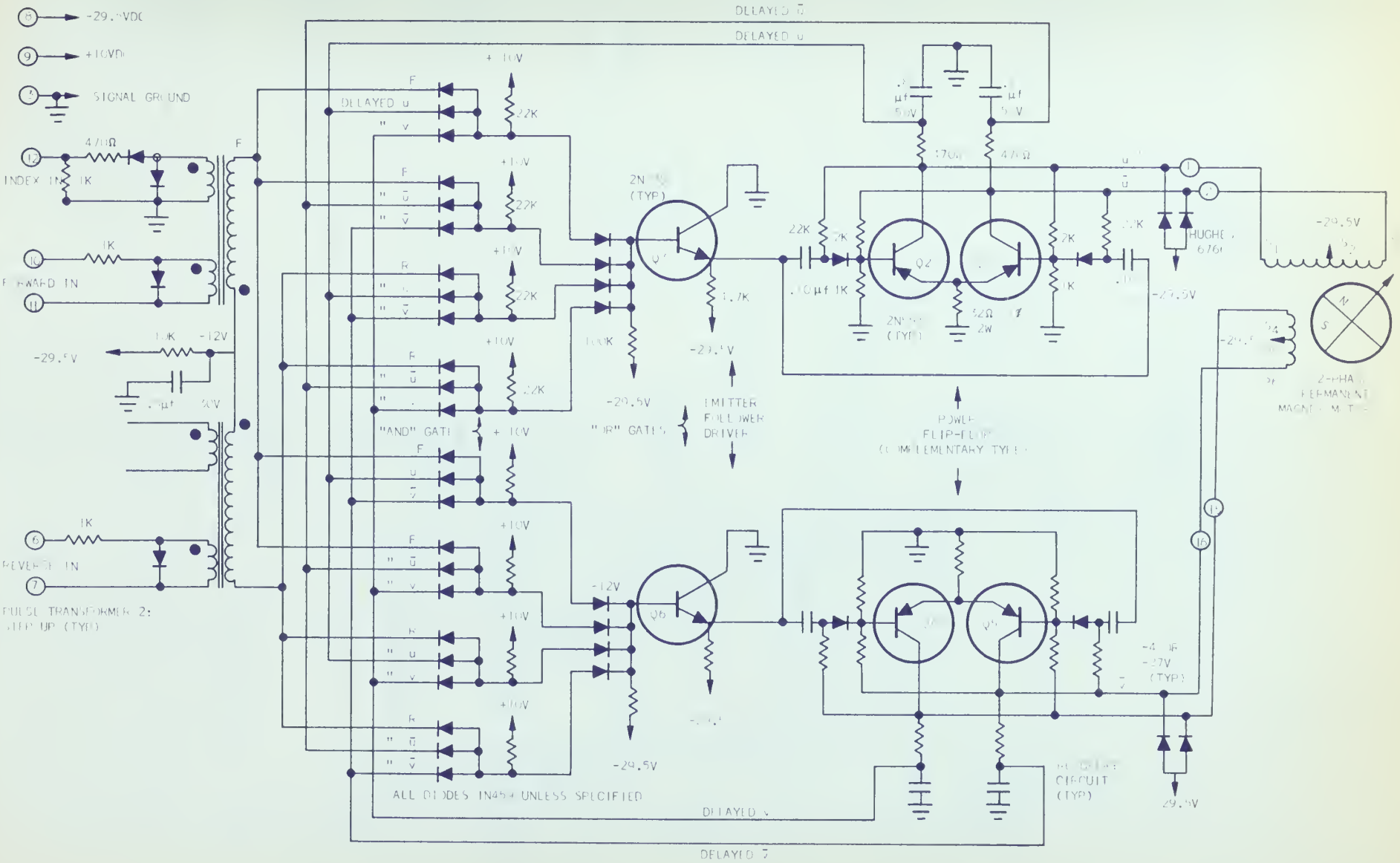

Figure 1. Stepper Motor Drive Logic Circuit Schematic

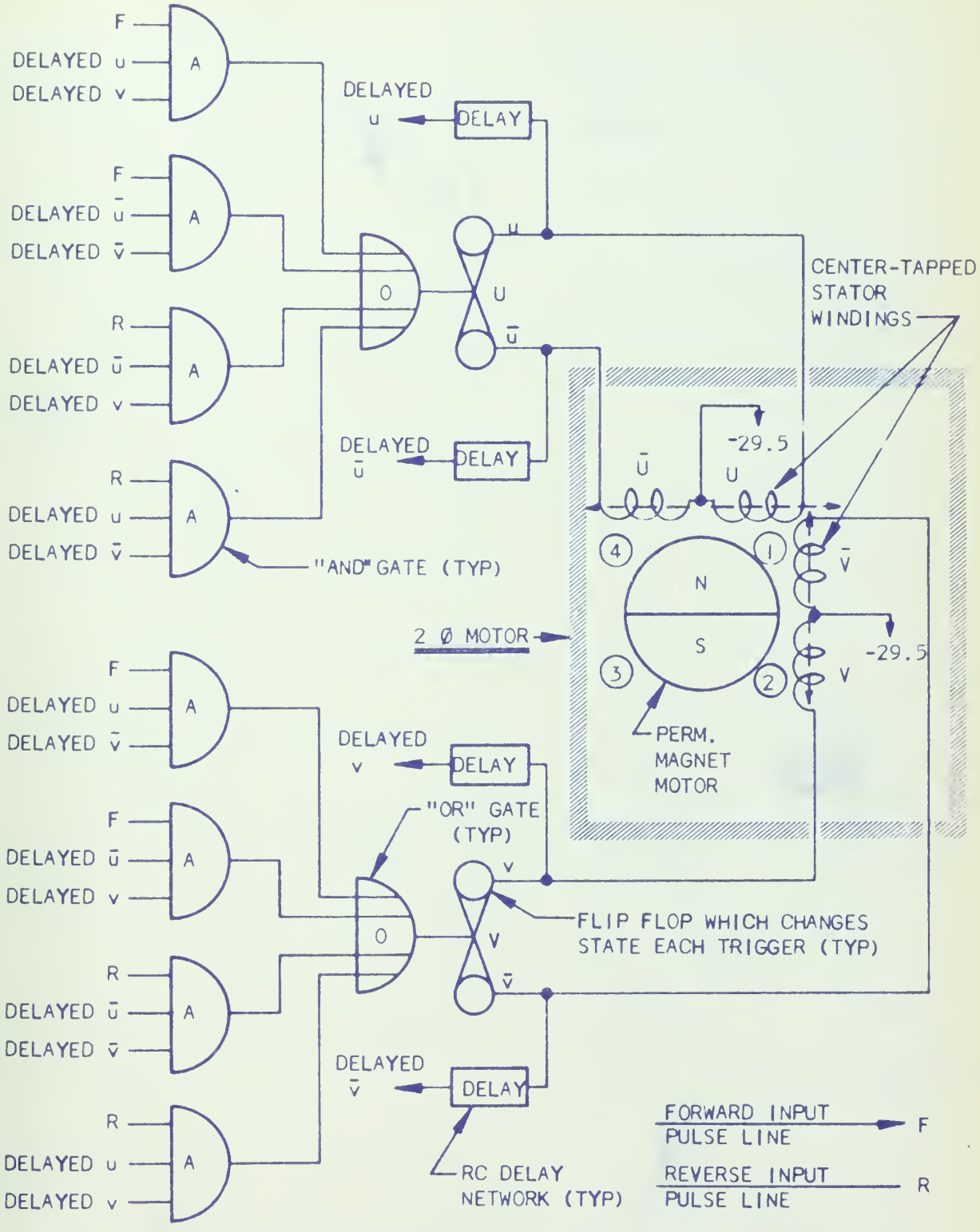

Figure 2 Stepper Motor Drive Logic Diagram

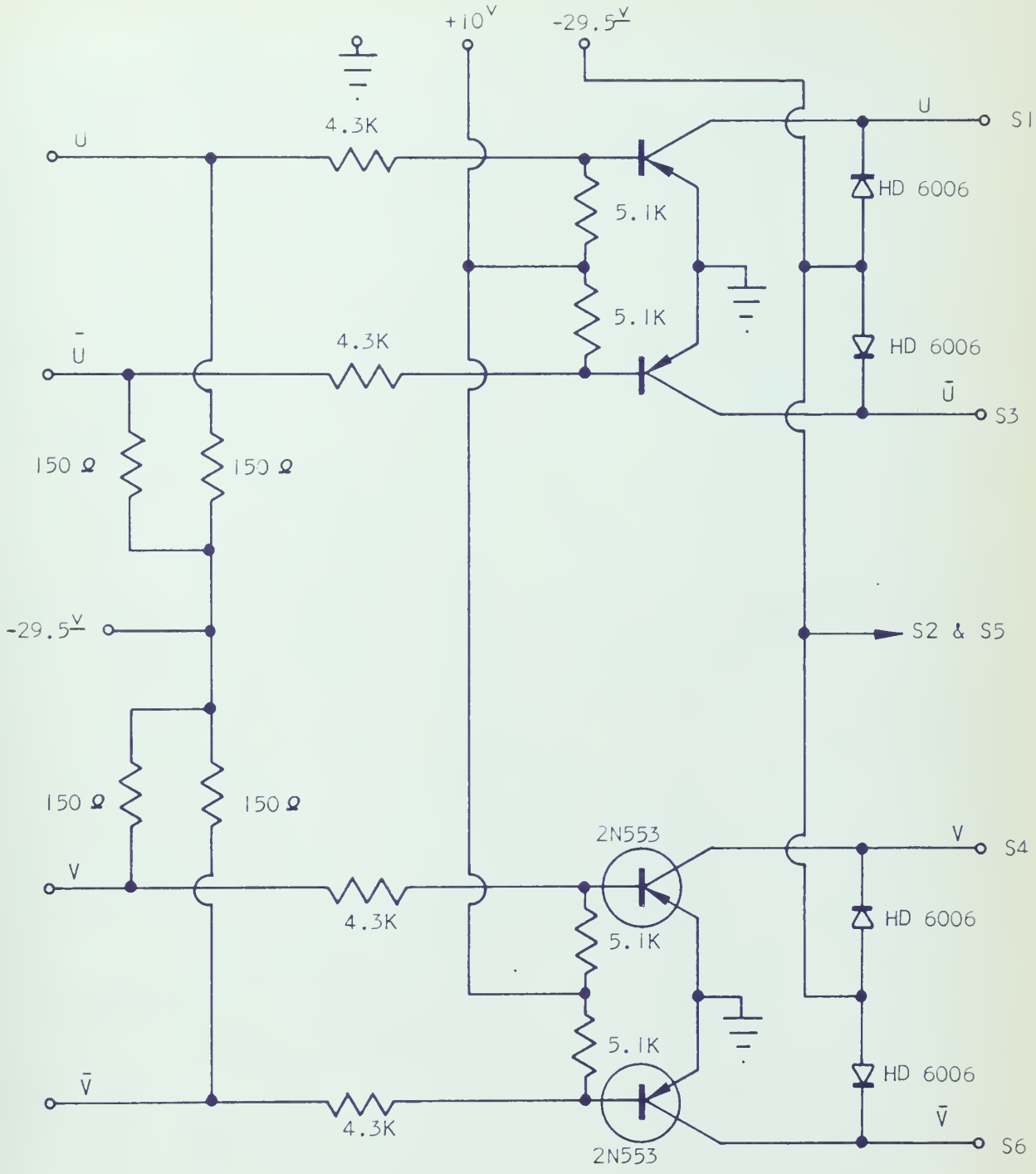

Figure 3 Power Gate Isolation for Logic Circuit

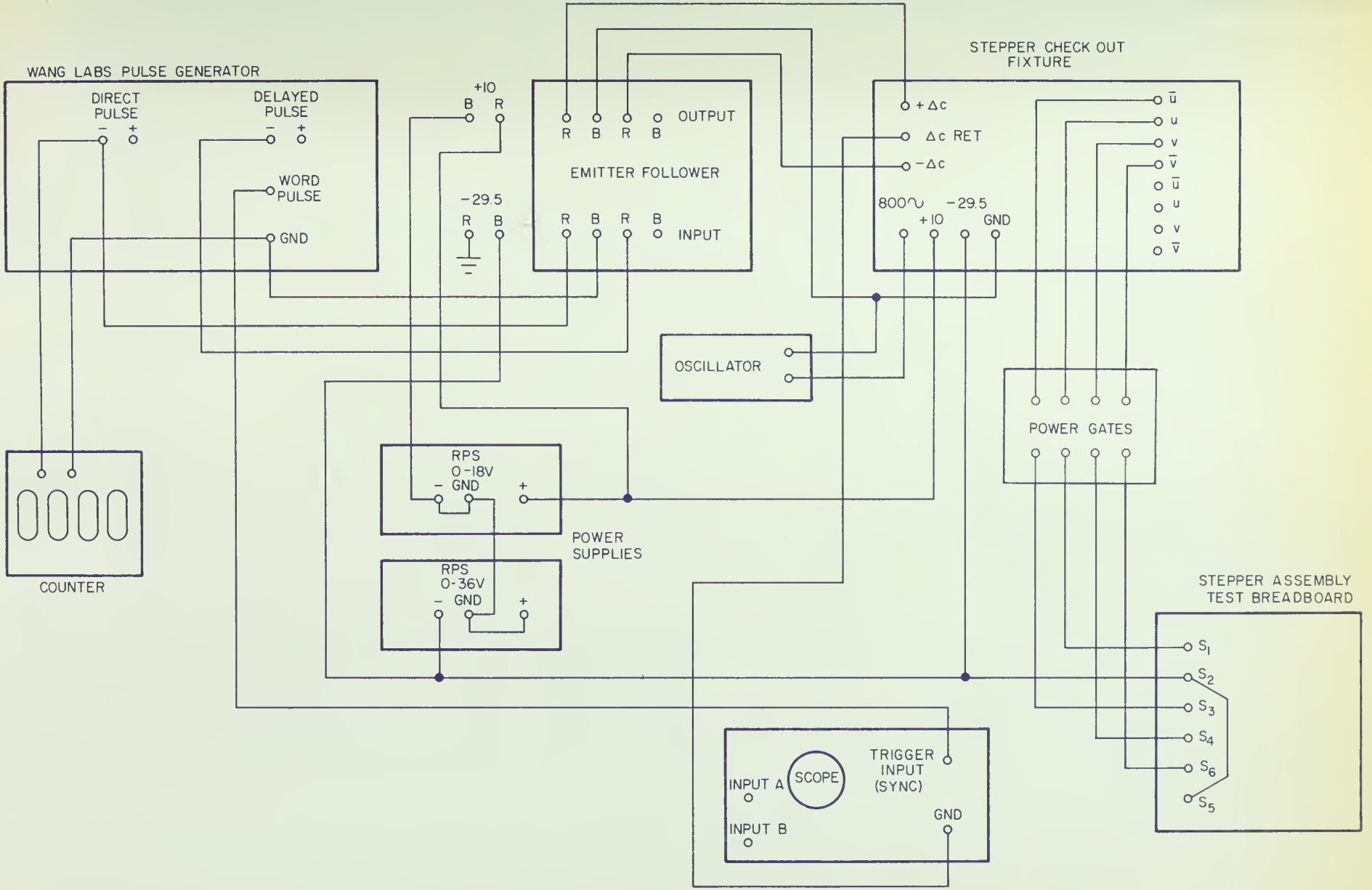

FIGURE. 4
BLOCK DIAGRAM OF TEST ASSEMBLY.

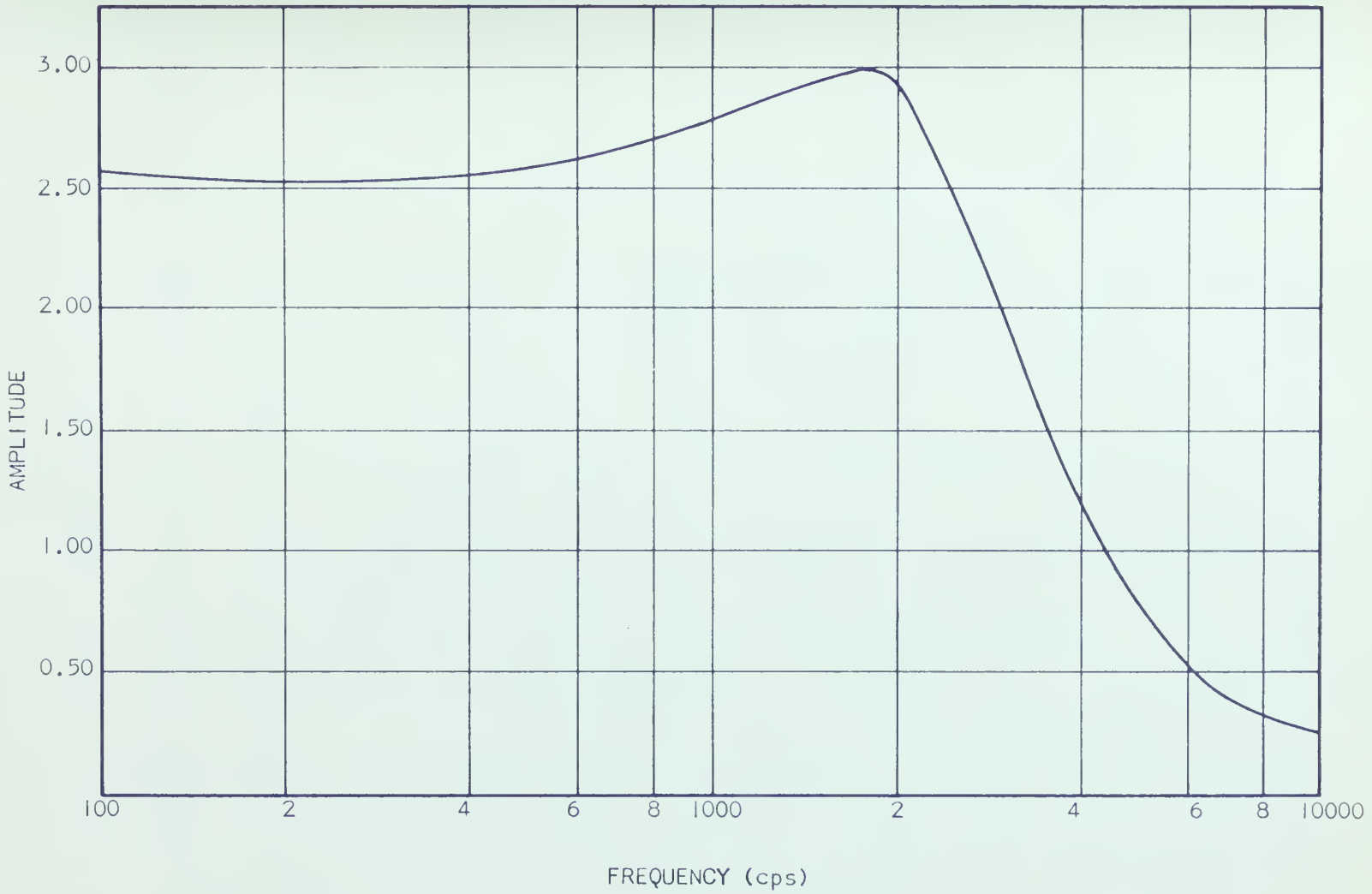

Figure 5 Midwestern Recorder Frequency Response

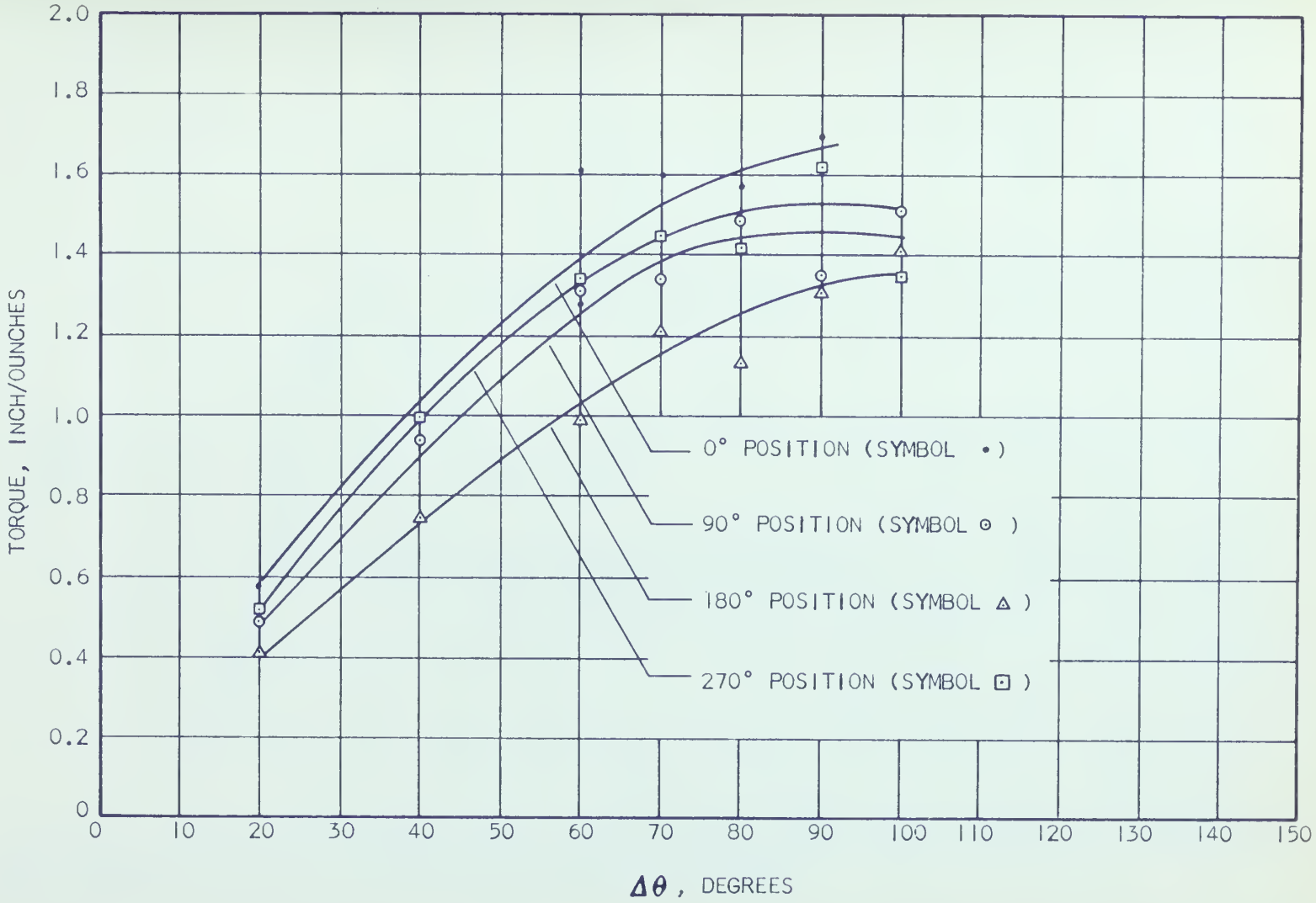

Figure 6 Static Torque Tests of Size 11 Stepper Motor with -29.5 volts on Stator

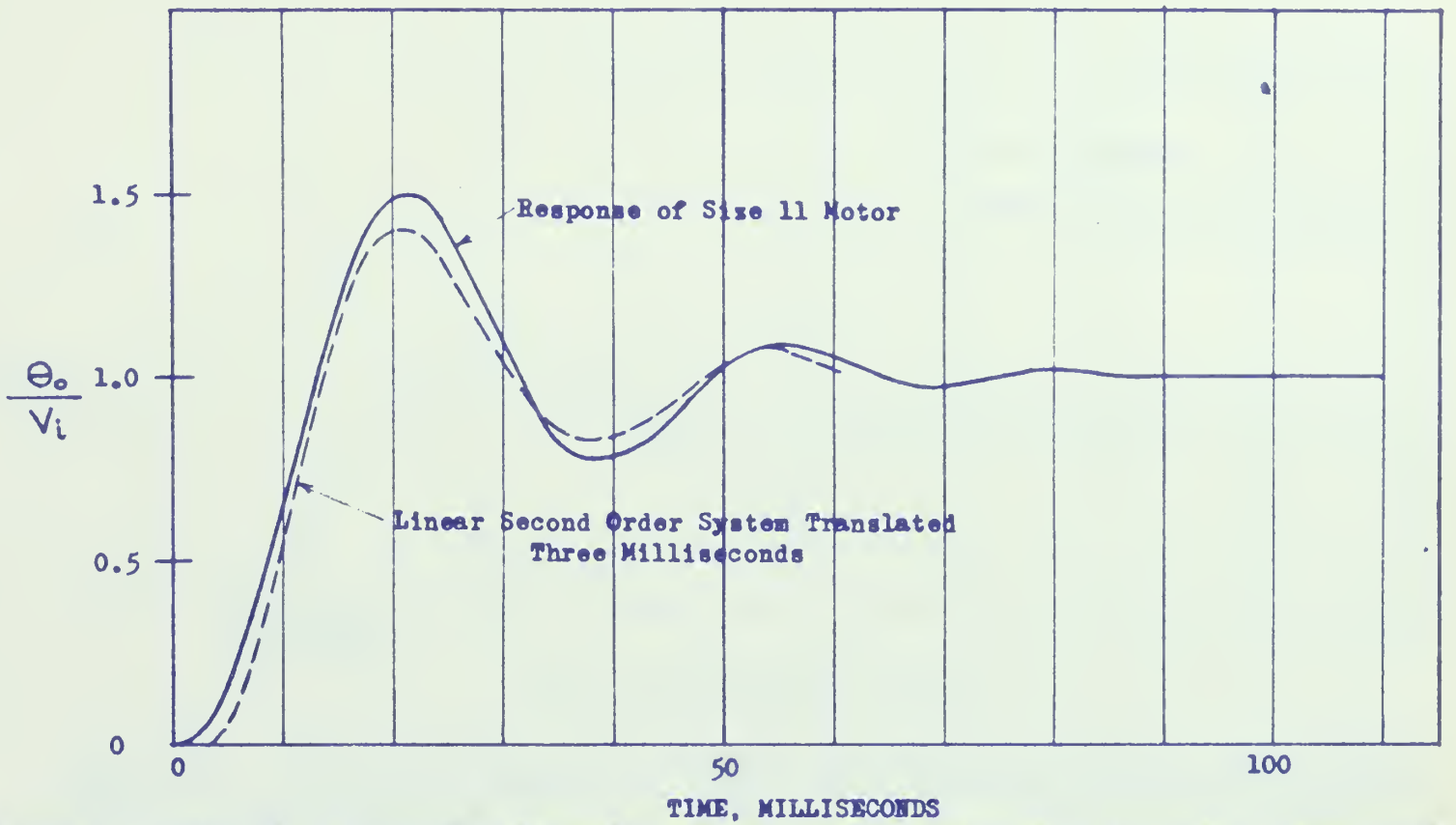

Figure 7 Comparison of Transient Response to a Step Input of the Size 11 Motor and a Theoretical Linear Second Order System ($\zeta = 0.27$, $\omega_n = 188.1$ radians/sec.)

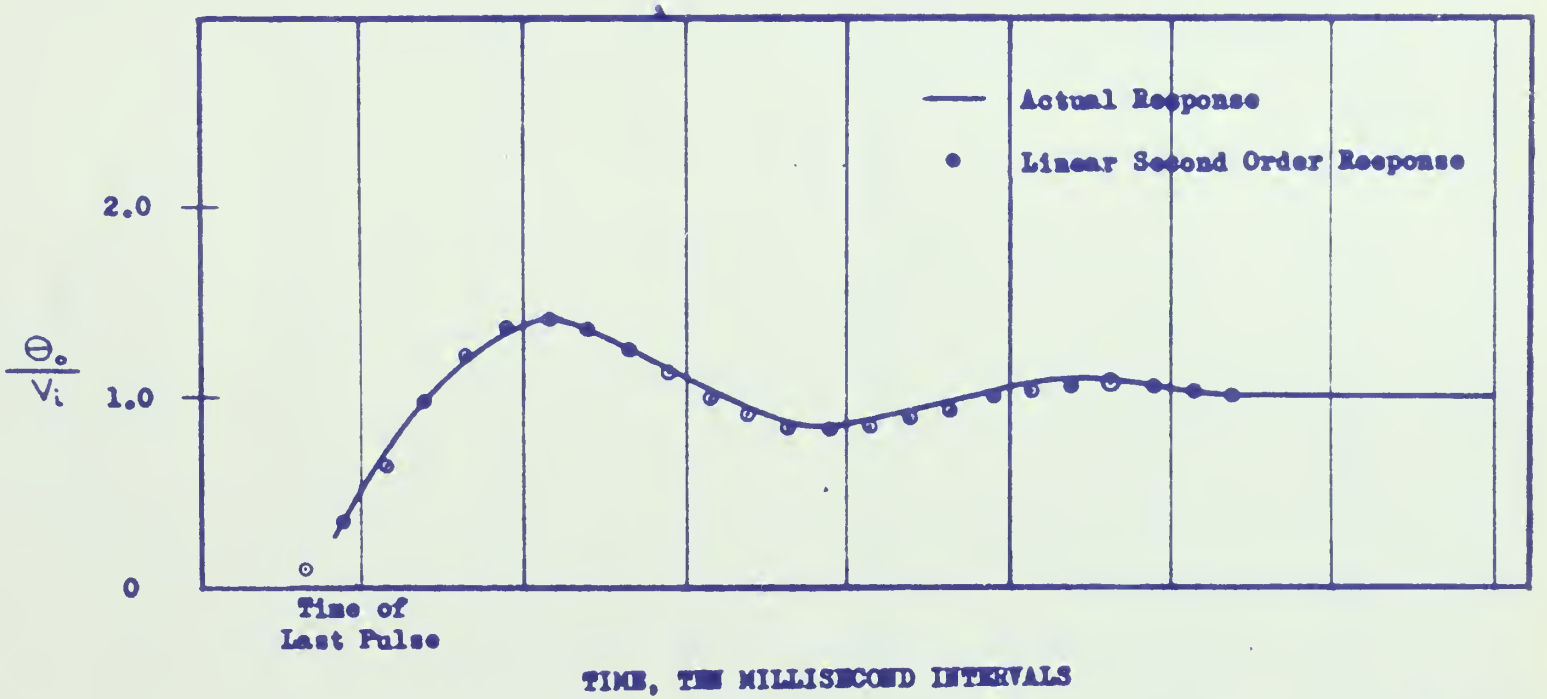

Figure 7A Comparison of Transient Response to the Last Reverse Pulse of a Four Forward - Four Reverse Pulse Train and Response of a Linear Second Order System Suitably Modified to Adjust for Initial Conditions.

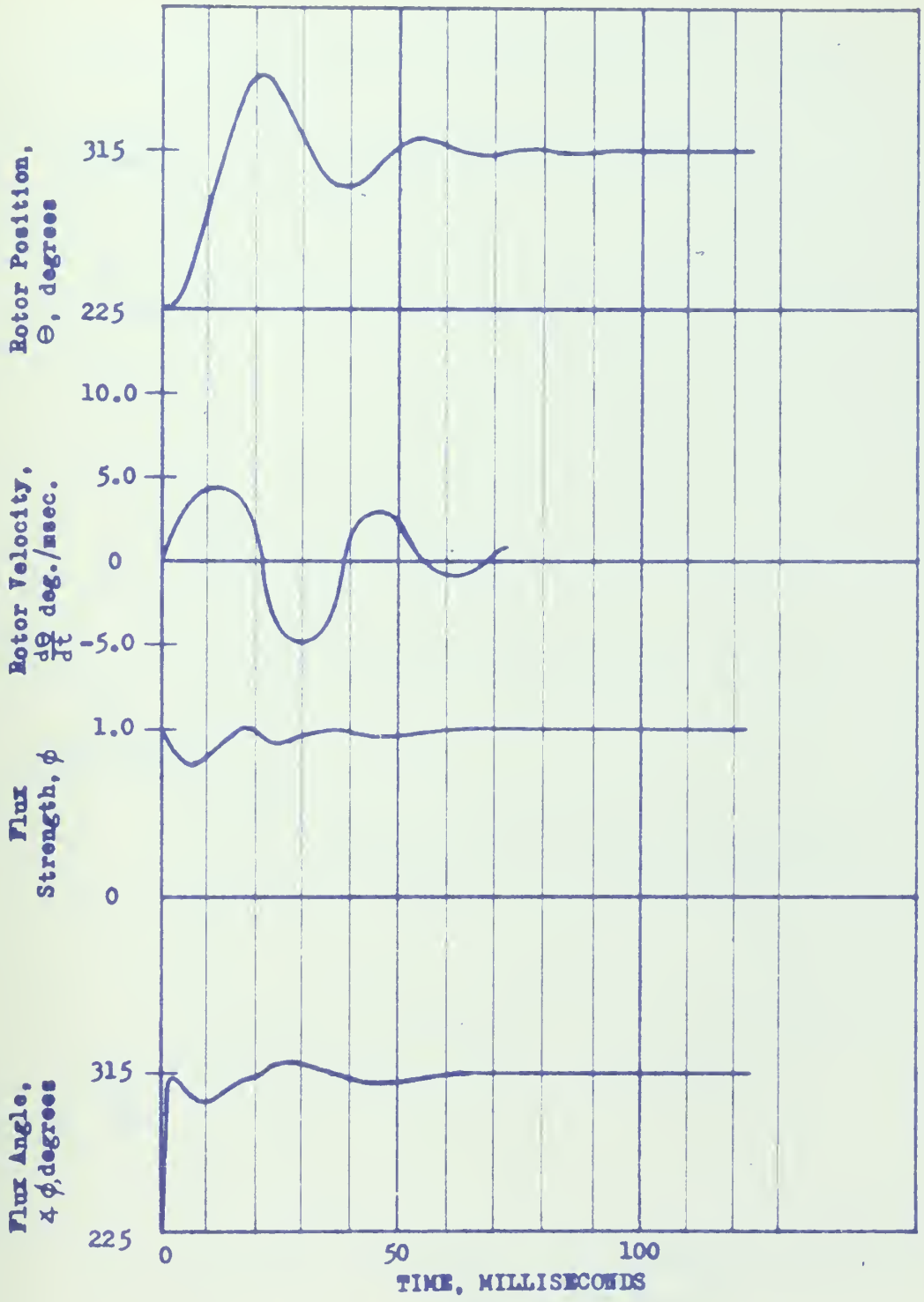

Figure 8 Motor Profile Responses to a Step Input, Size 11

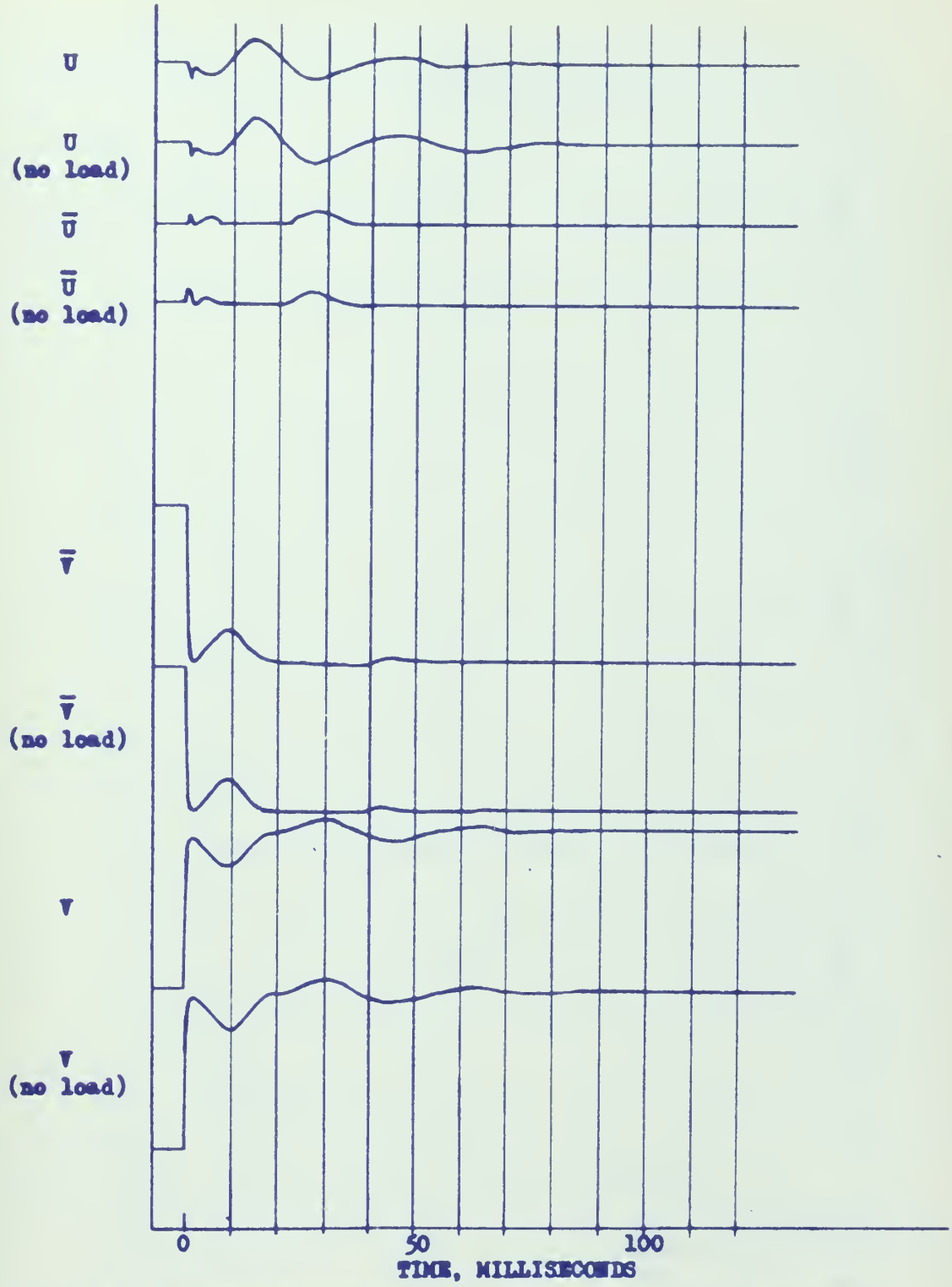

Figure 8A Current Responses to a Step Input, Size 11, Showing Comparison of No Load Currents and Currents with Load of Resolver and Anti-Backlash Gear Train (70.6:1)

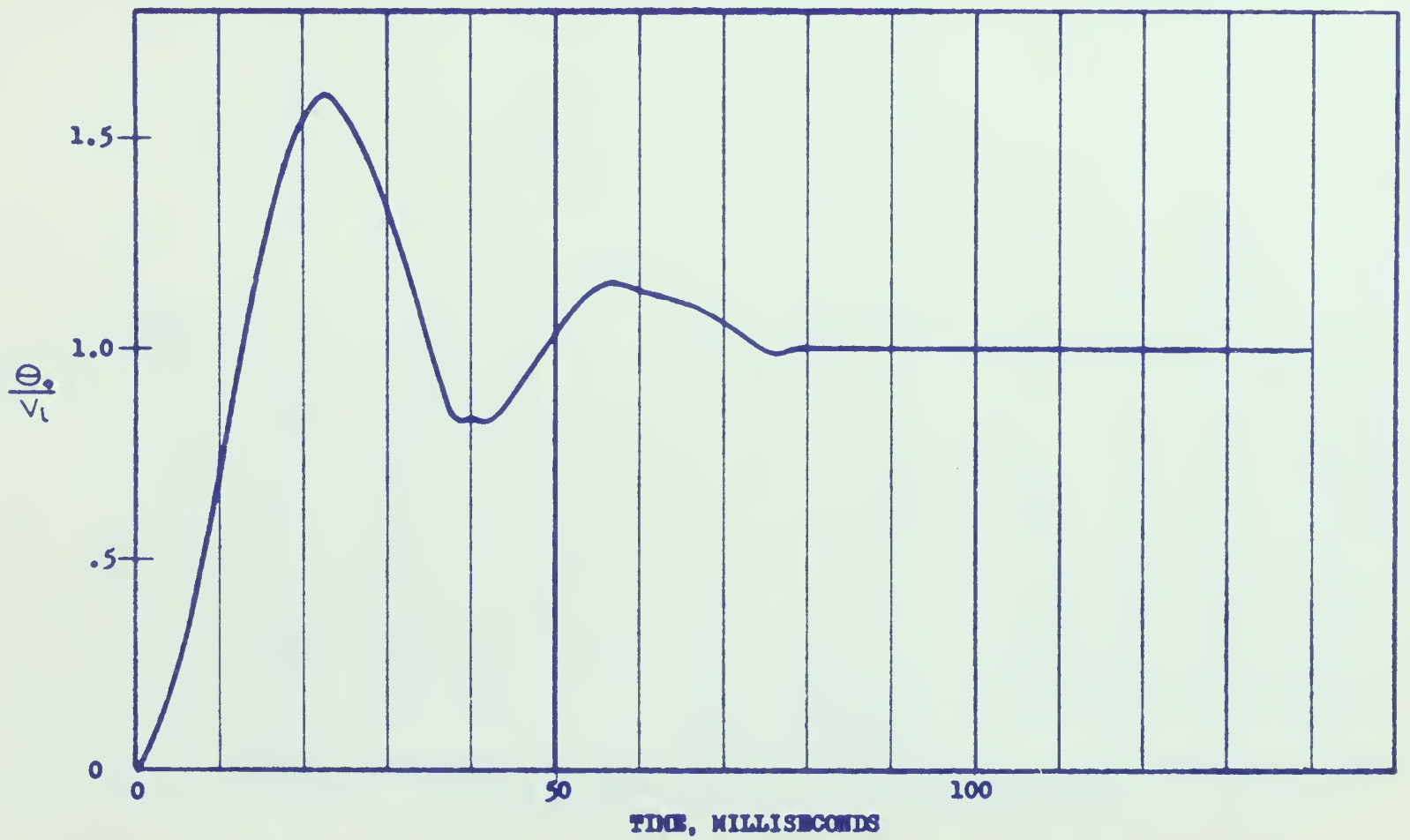

Figure 9 Transient Response to Step Input for Size 11 Motor without Anti-Backlash Gears.

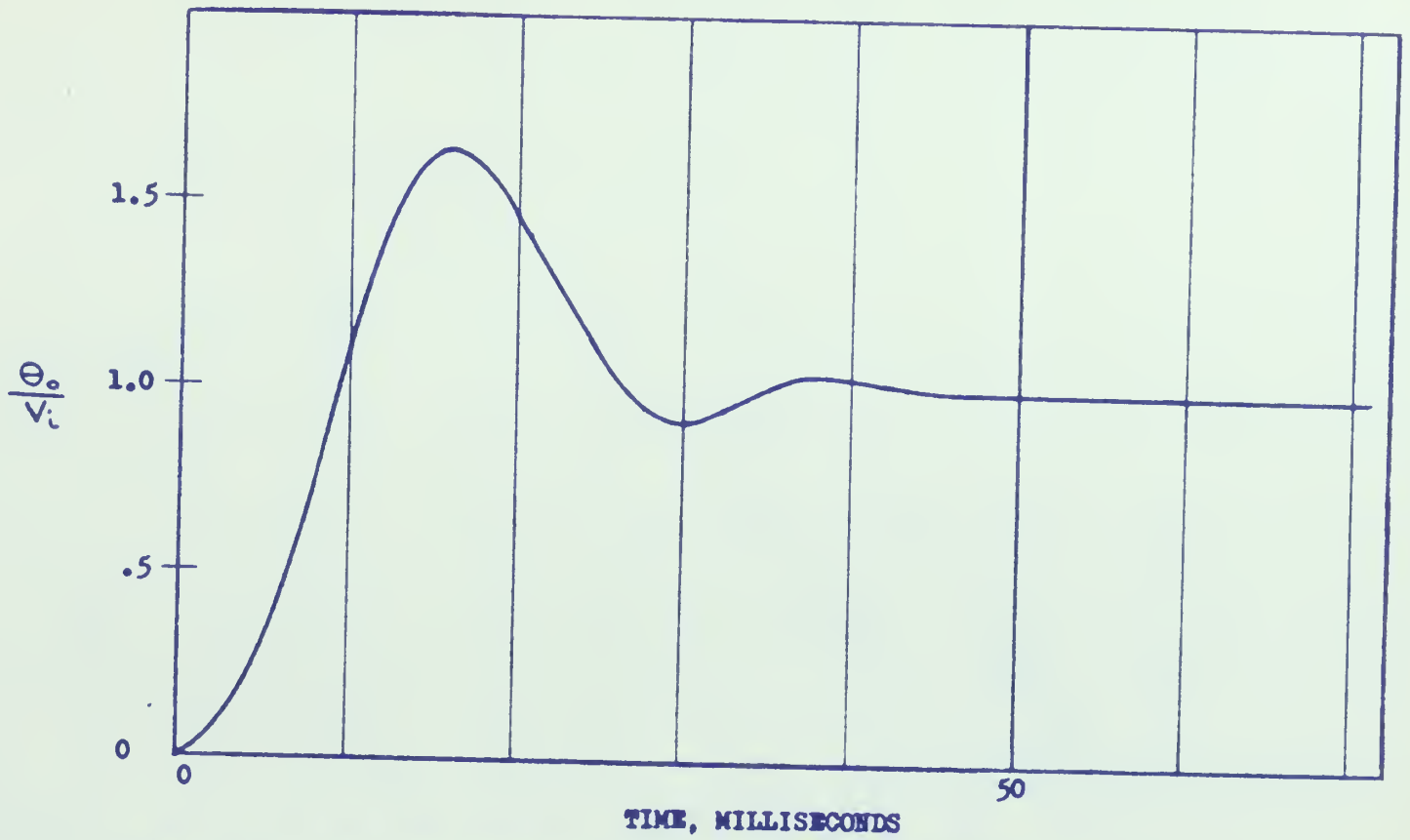

Figure 10 Transient Response of Size 8 Motor to a Step Input

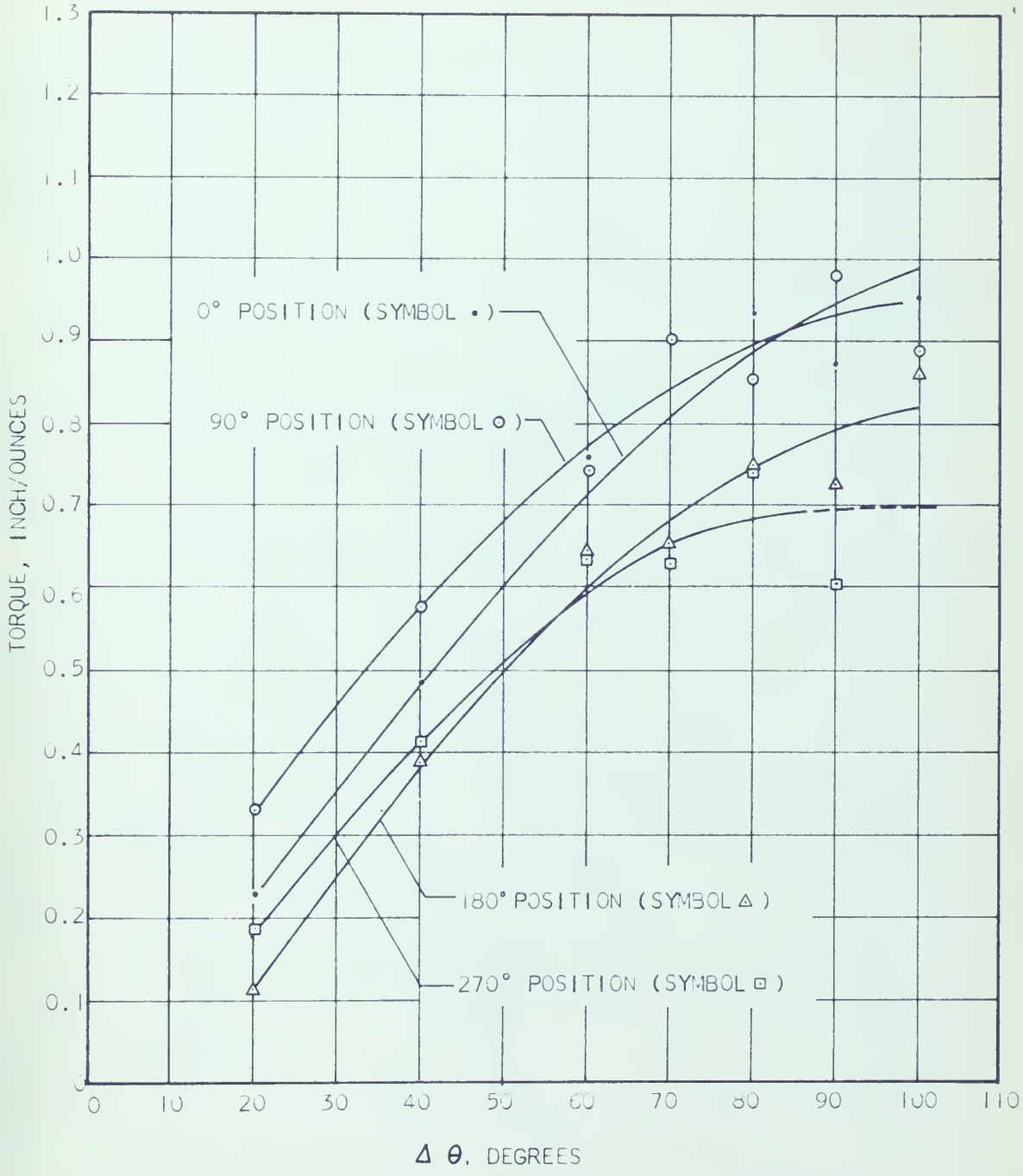

Figure 11 Static Torque Tests of Size 8 Stepper Motor with -29.5 Volts on Stator

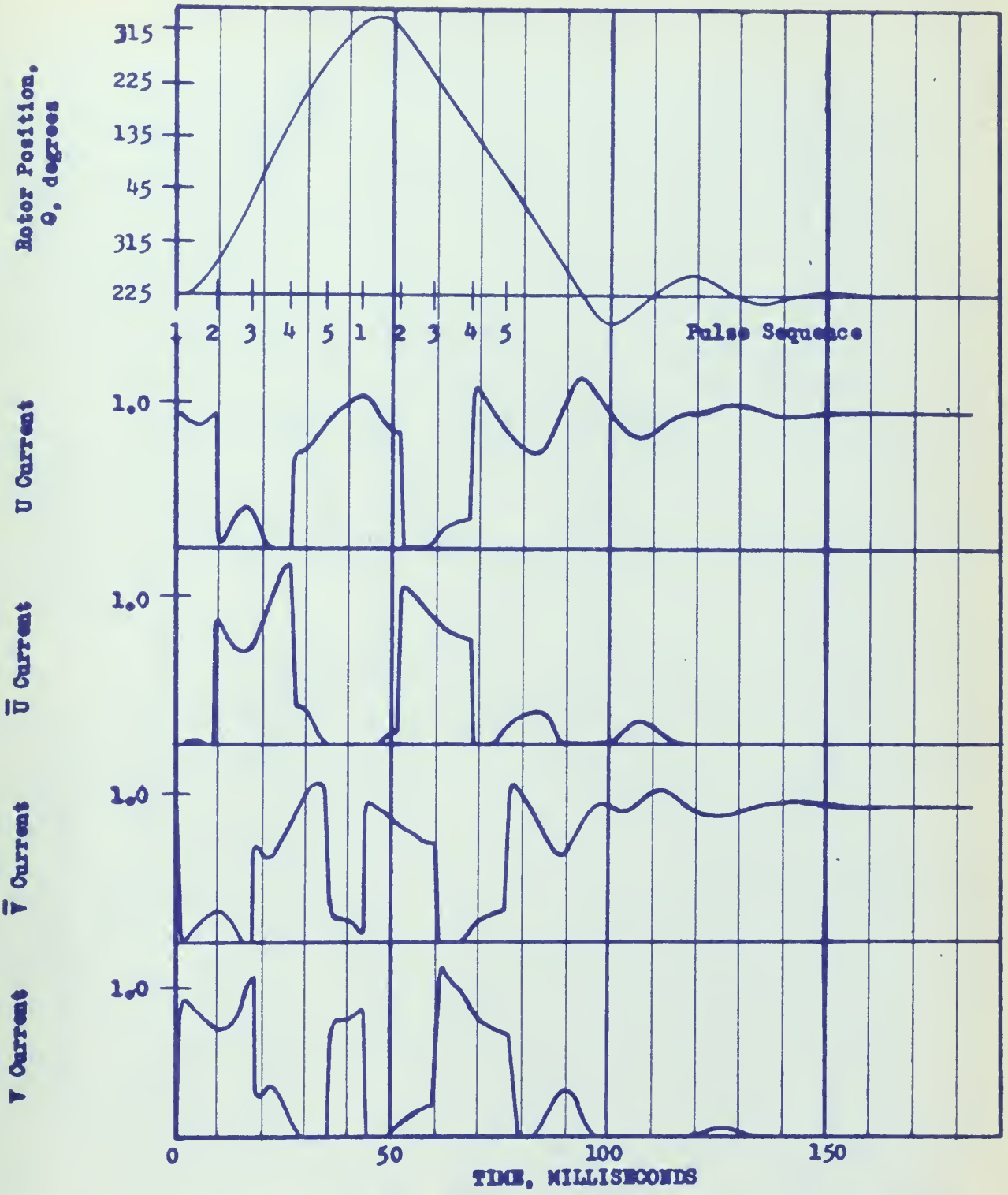

Figure 12 Size 11 Motor Response to 5 fwd.-5 rev. pulse train, showing (top to bottom) Rotor Position and each current just prior to motor failure.

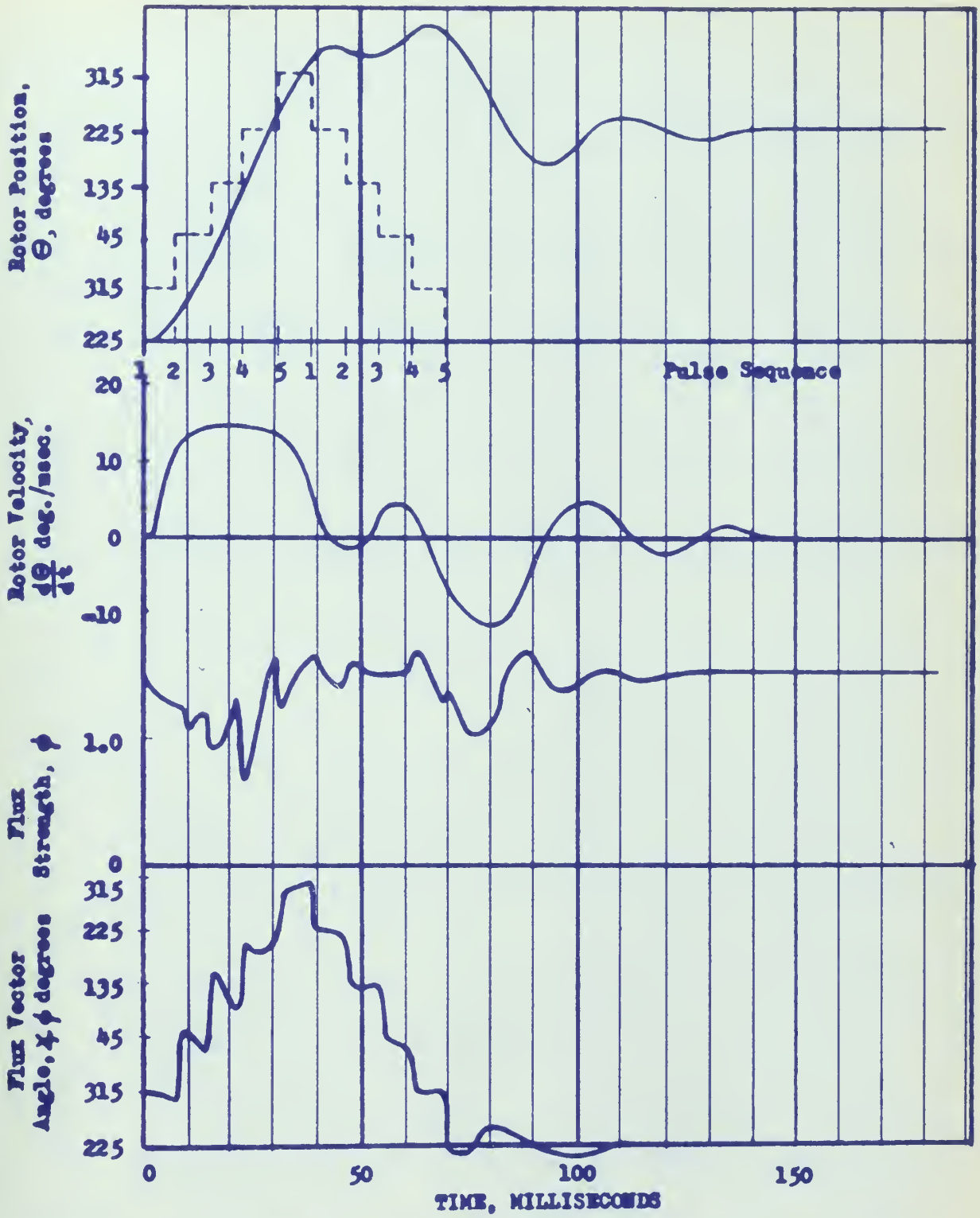

Figure 13 Size 11 Motor response to 5 fwd.-5 rev. pulse train showing failure profile.

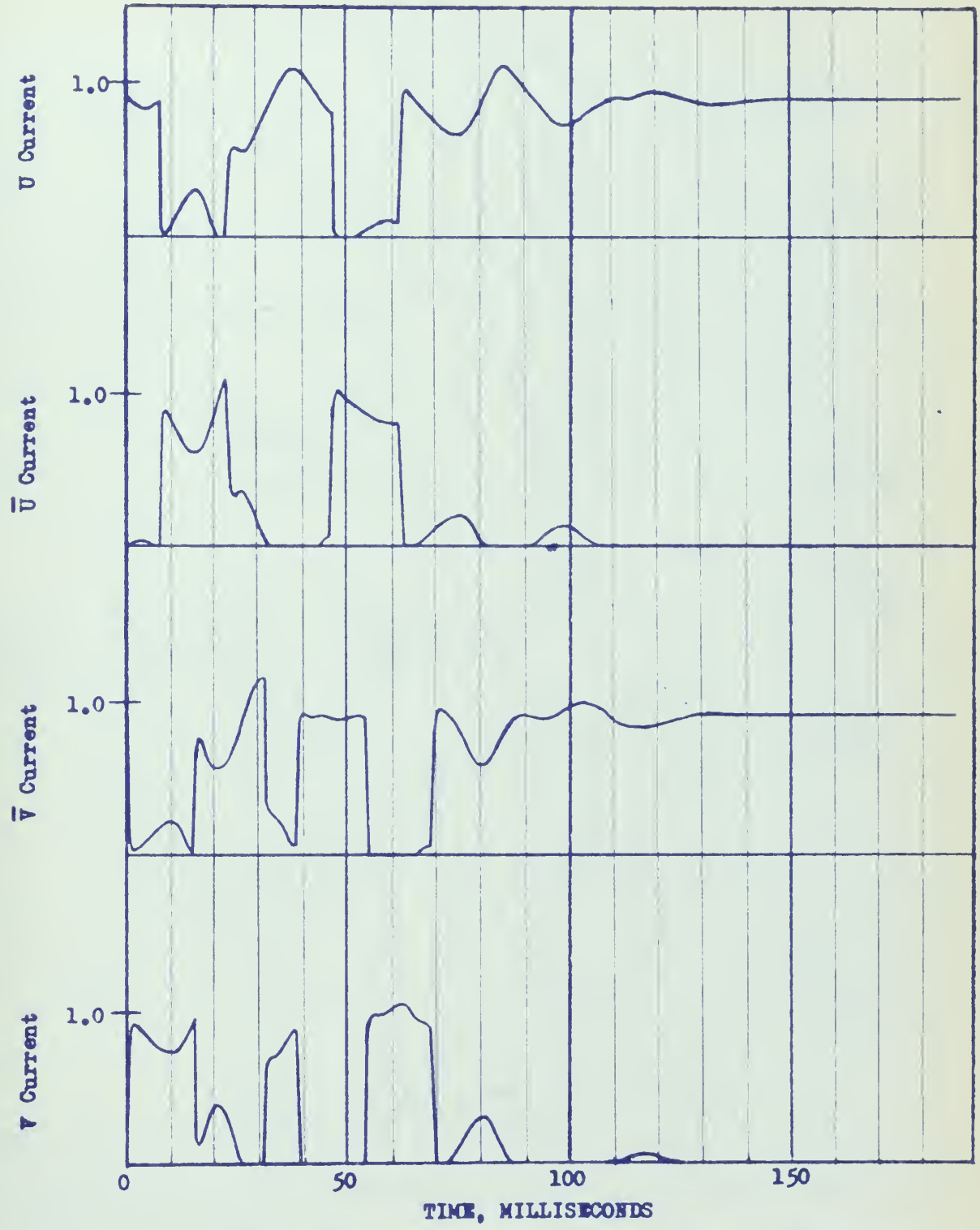

Figure 14 Size 11 Motor response to 5 fwd.-5 rev. pulse train showing all currents at failure.

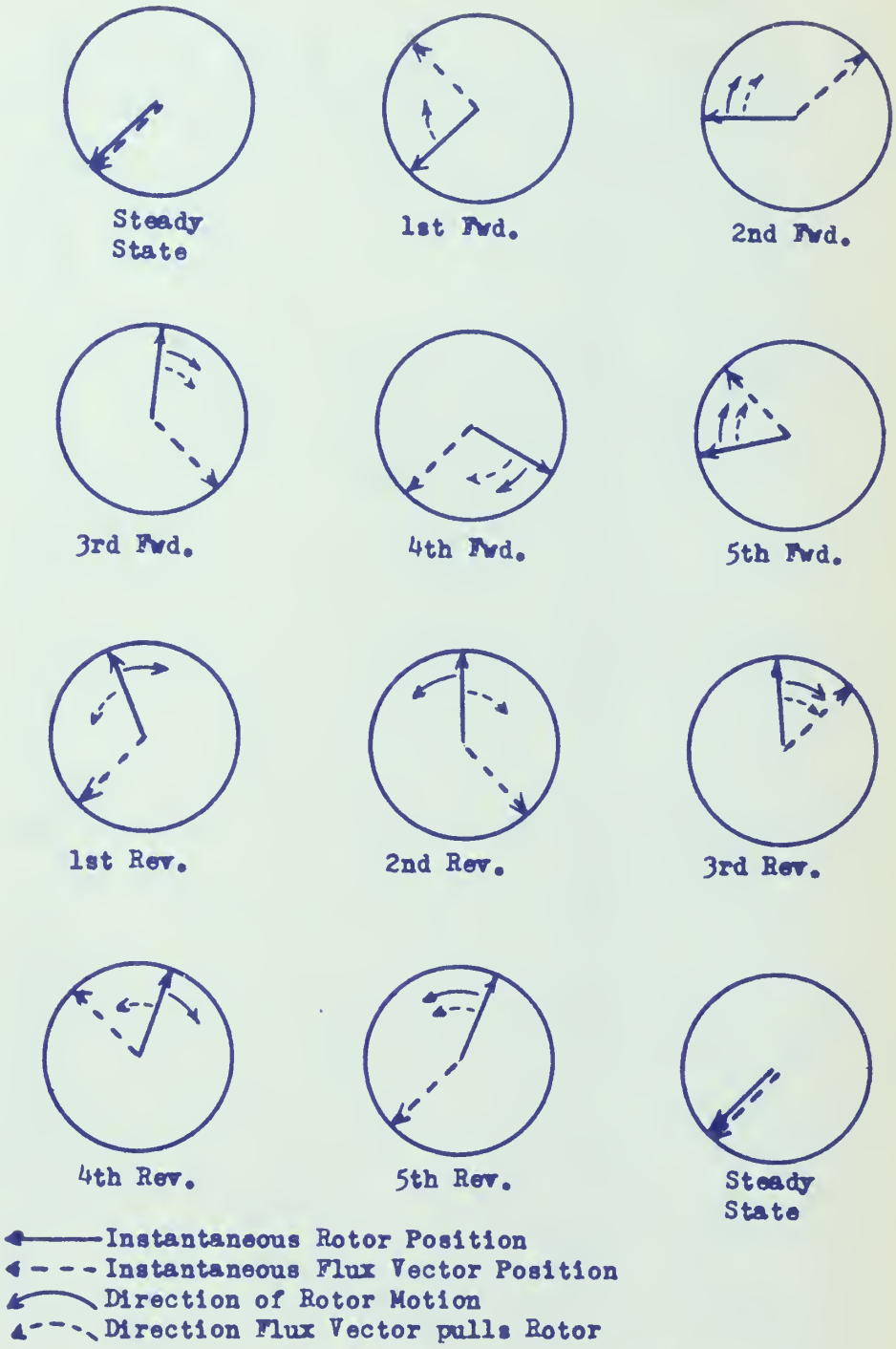

Figure 15 Size 11 Motor Rotor and Resolved Flux Vector Positions for 5 fwd.-5 rev. program failure.

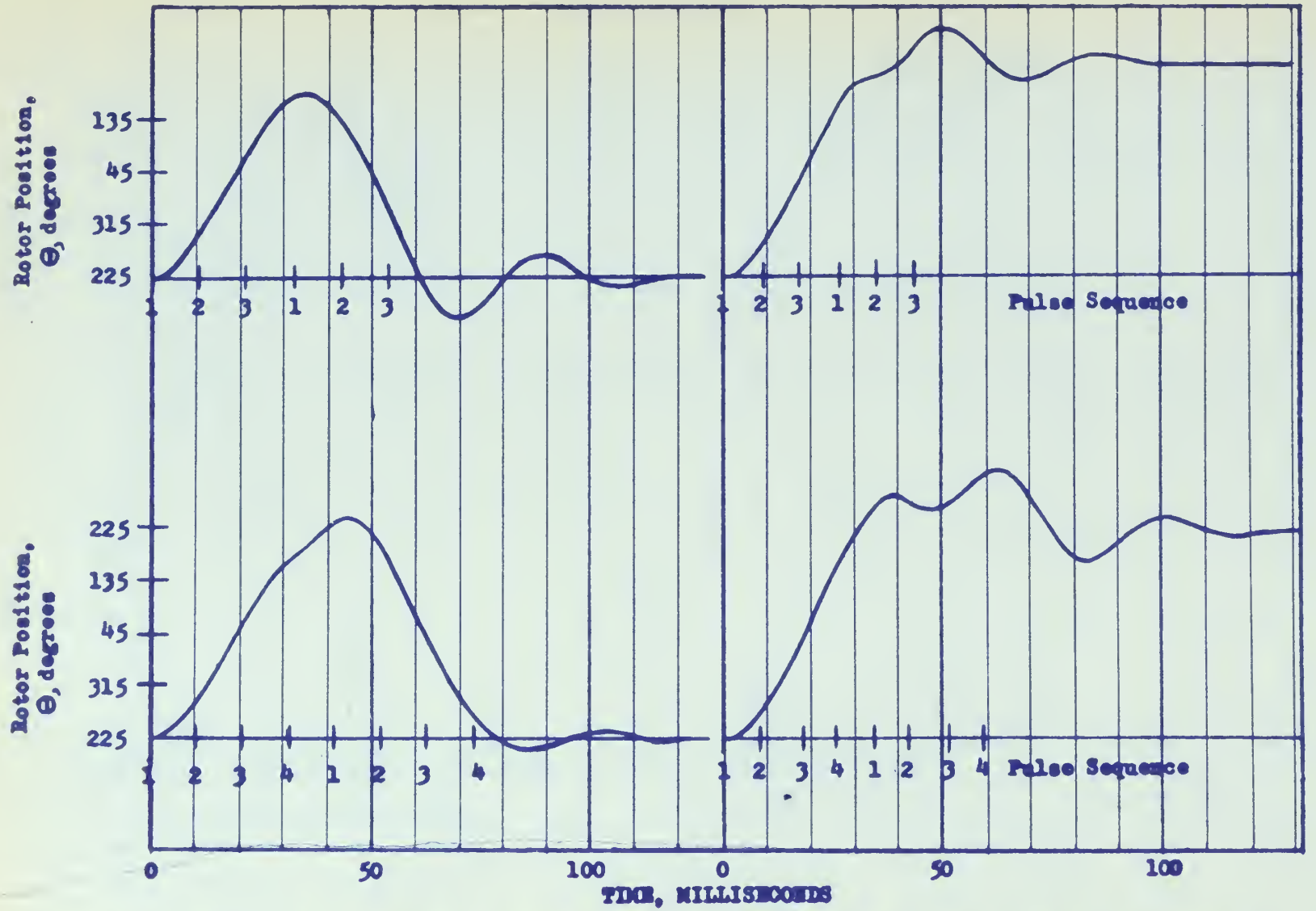

Figure 16 Size 11 Motor responses showing Rotor Position for: Top Left: 3 fwd.-3 rev. program just before failure; Top Right: 3 fwd.-3 rev. program at failure; Bottom Left: 4 fwd.-4 rev. program just before failure; Bottom Right: 4 fwd.-4 rev. program at failure.

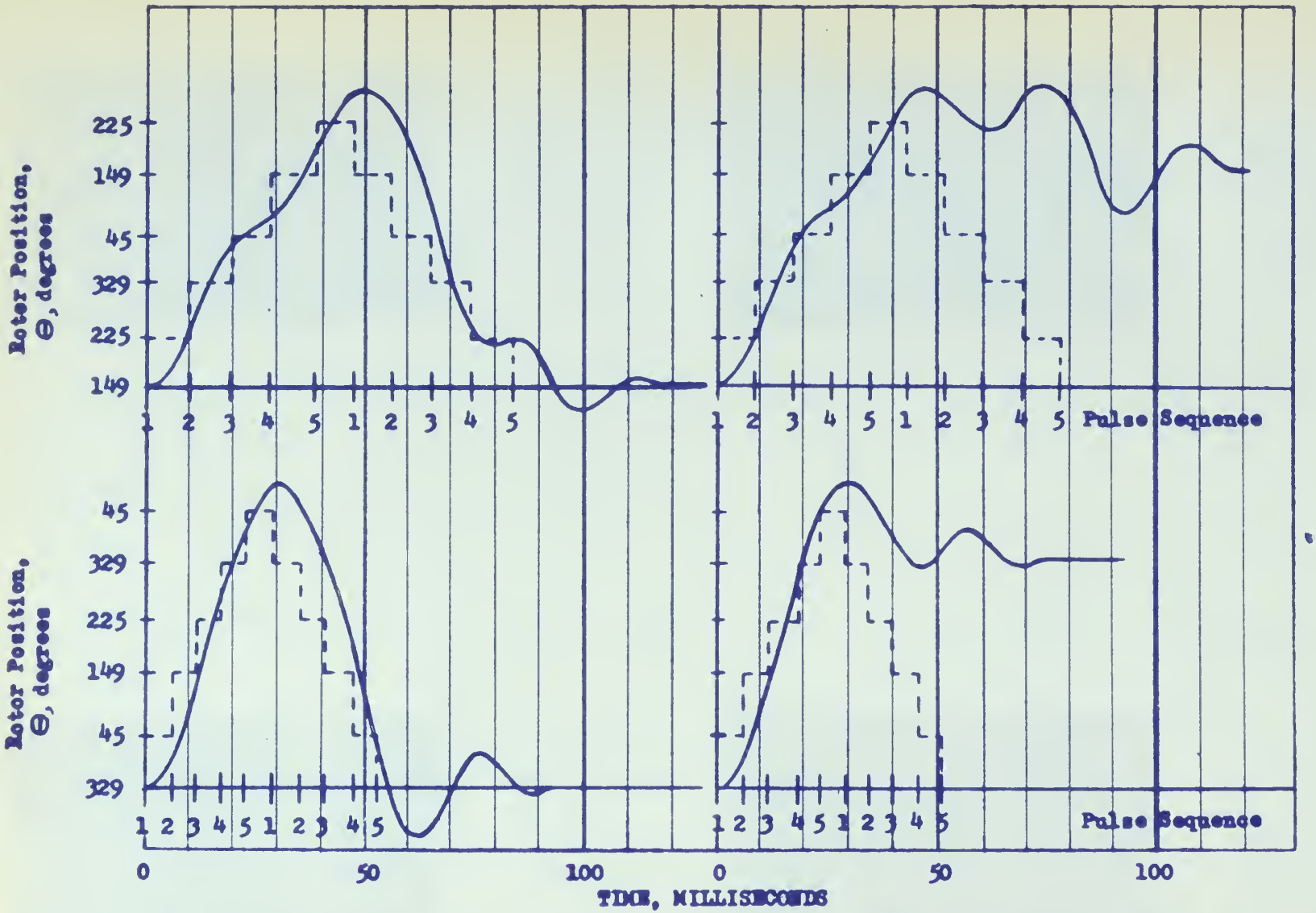

Figure 17 Size 8 Motor responses to 5 fwd.-5 rev. program showing Rotor Position: Top Left: just before anomalous failure; Top Right: at anomalous failure; Bottom Left: just before "normal" failure; Bottom Right: at "normal" failure.

Appendix A

Logic Circuit Response to Various Pulse Programs Using 150-ohm Resistors to Simulate Stepper Motor Loading.

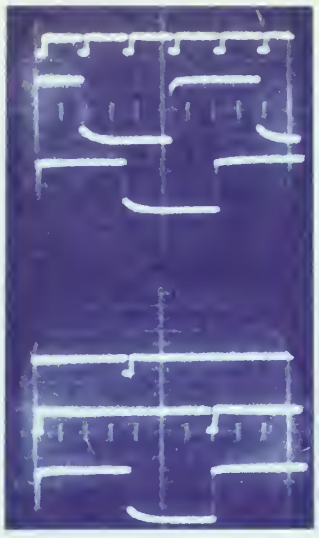

Photo. 1
Top: 1-Forward-Pulse Train
$\overline{U}$ State, $\overline{V}$ State at
567 p.p.s. 1 ms/cm
Bottom: 1-Forward-Pulse Train
1-Reverse-Pulse Train
$\overline{V}$ State at 288 p.p.s.
1 ms/cm

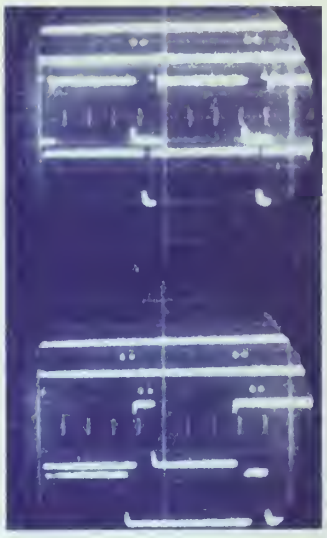

Photo. 2
2-Forward-Pulse Train
2-Reverse-Pulse Train
$\overline{U}$ State, $\overline{V}$ State about
295 p.p.s, 10 ms/cm
Top: Before Logic Circuit Failure
Bottom: After Logic Circuit Failure

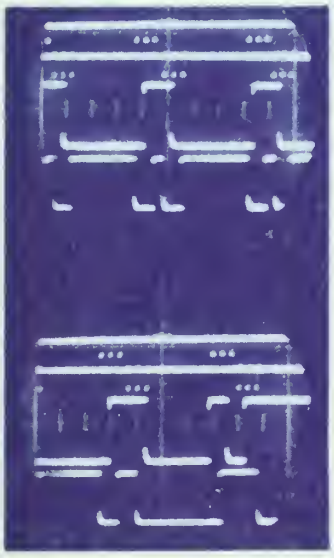

Photo. 3
3-Forward-Pulse Train
3-Reverse-Pulse Train
$\overline{U}$ State, $\overline{V}$ State about
300 p.p.s., 10 ms/cm
Top: Before Logic Circuit Failure
Bottom: After Logic Circuit Failure

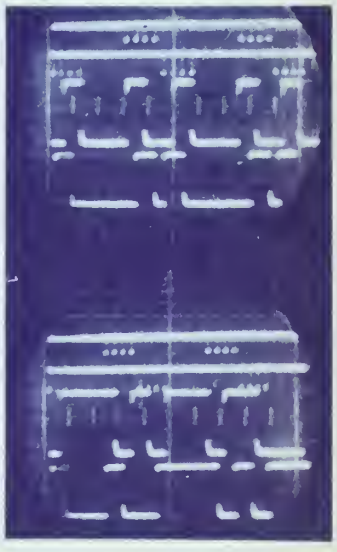

Photo. 4
4-Forward-Pulse Train
4-Reverse-Pulse Train
$\overline{U}$ State, $\overline{V}$ State about
300 p.p.s., 10 ms/cm
Top: Before Logic Circuit Failure
Bottom: After Logic Circuit Failure

Appendix A

Logic Circuit Response to Various Pulse Programs Using 150-ohm Resistors to Simulate Stepper Motor Loading.

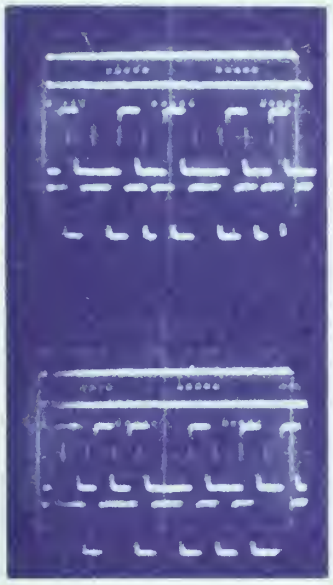

Photo. 5
5-Forward-Pulse Train
5-Reverse-Pulse Train
$\overline{U}$ State, $\overline{V}$ State about
310 p.p.s., 10 ms/cm
Top: Before Logic Circuit Failure
Bottom: After Logic Circuit Failure

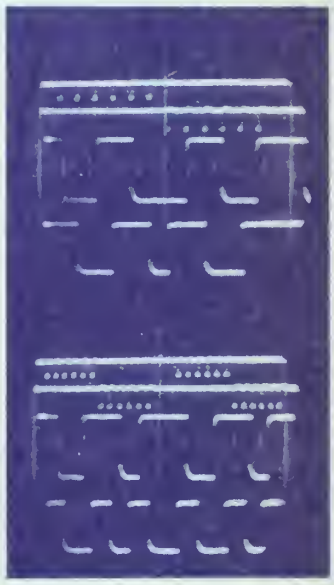

Photo. 6
6-Forward-Pulse Train
6-Reverse-Pulse Train
$\overline{U}$ State, $\overline{V}$ State about
396 p.p.s., 5 ms/cm
Top: Before Logic Circuit Failure
Bottom: After Logic Circuit Failure

Appendix A

Transient Responses of Size 11 Motor with Anti-Backlash Gearing

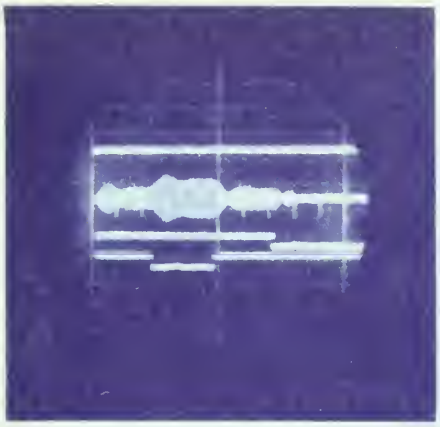

Photo. 7
2-Forward-Pulse Train
2-Reverse-Pulse Train
13.7 p.p.s., 30 millisec/cm

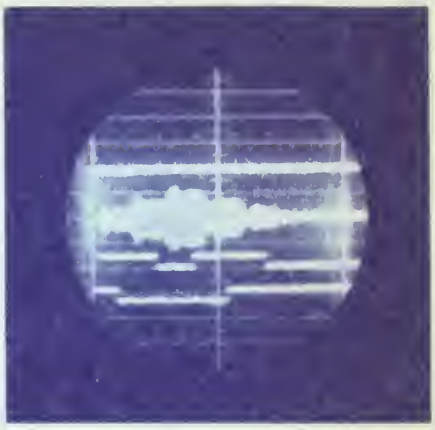

Photo. 8
3-Forward-Pulse Train
3-Reverse-Pulse Train
13.7 p.p.s., 50 millisec/cm

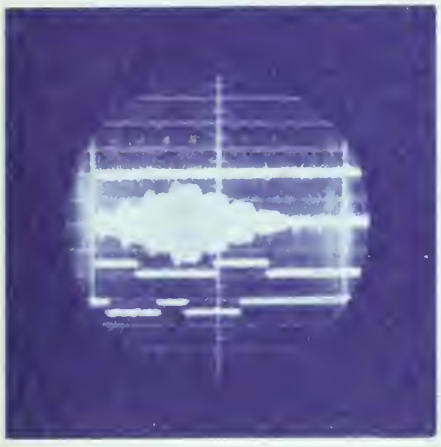

Photo. 9
4-Forward-Pulse Train
4-Reverse-Pulse Train
13.7 p.p.s., 70 millisec/cm

Photo. 10
5-Forward-Pulse Train
5-Reverse-Pulse Train
12 p.p.s., 100 millisec/cm

NOTE: Photos. 7 through 10 Show the Combined Pulse Train, Resolver Output, V State, U State in that Order

Appendix A

Comparison of Response of Size 11 Motor Using Anti-Backlash Gearing with or without Power Gates.

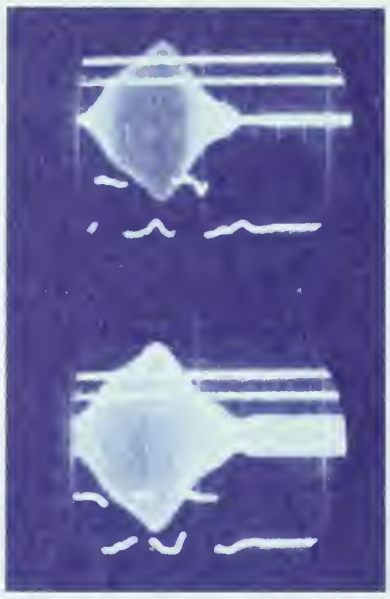

Photo. 11
Response to 5-Forward-Pulse, 5-Reverse-Pulse Train Showing Large Back EMF Hump in $\overline{U}$ State (top) and Change in $\overline{U}$ Logic State as a Result of Back EMF (bottom). At 76 p.p.s., 20 ms/cm.

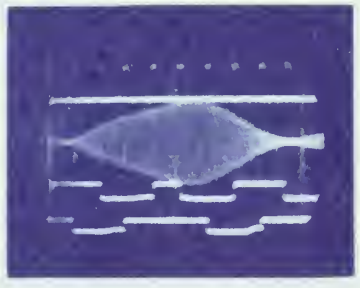

Photo. 12
Response to 5-Forward-Pulse, 5-Reverse-Pulse Train Showing How Power Gate Isolation Completely Eliminates Back EMF Reflected into the Logic Circuit. Shown are the Combined Pulse Train, the Resolver Output, $\overline{V}$ State, $\overline{U}$ State

Appendix A

Comparison of Response of Size 11 Motor with and without Power Gates. Also Indicating the Desirability of Anti-Backlash Gears.

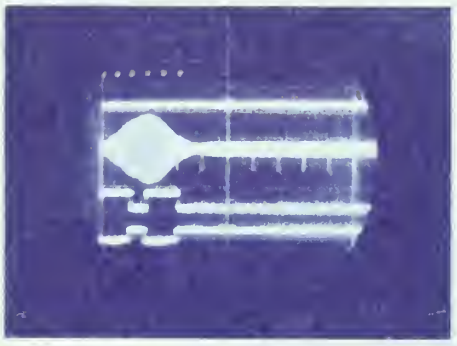

Photo. 13
3-Forward-Pulse Train, 3-Reverse-Pulse Train with Anti-Backlash Gears and Power Gates

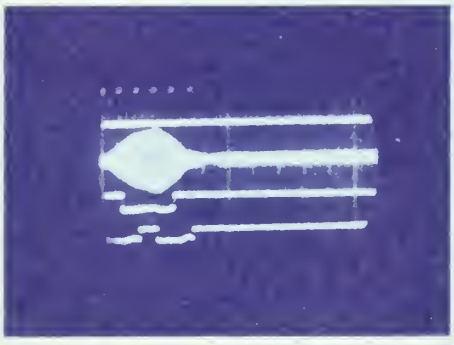

Photo. 14
3-Forward-Pulse Train, 3-Reverse-Pulse Train without Anti-Backlash Gears but with Power Gates

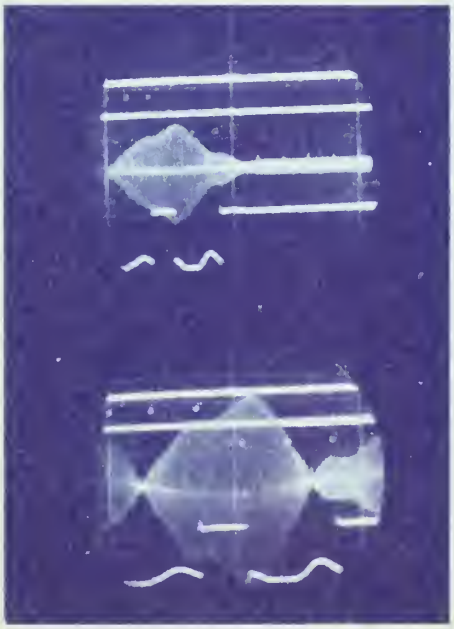

Photo. 15
3-Forward-Pulse Train, 3-Reverse-Pulse without Power Gates
Top: With Anti-Backlash Gears
Bottom: Without Anti-Backlash Gears

Appendix A

Comparison of Current and Voltage Decay Response in Size 11 Stepper Motor Rotor Winding

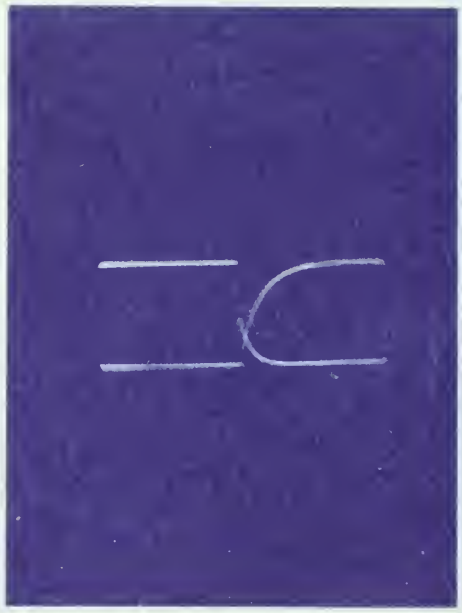

Photo. 16

Top: $\overline{V}$ Voltage (decaying exponential)
Bottom: V Current (rising exponential)

Appendix A

Current Response of Size 11 Stepper Motor to a Program of Four Forward Pulses Immediately Followed by Four Reverse Pulses Showing Induced EMF Effects

Anti-Backlash Gear Train
Pulse Spacing = 30.1 milliseconds

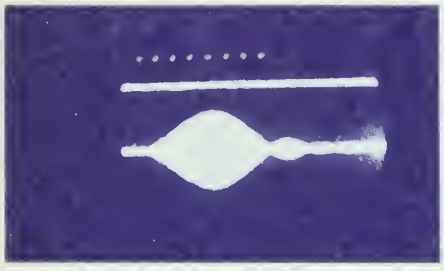

Photo. 17

Top: Combined Pulse Trains
Bottom: Resolver Output

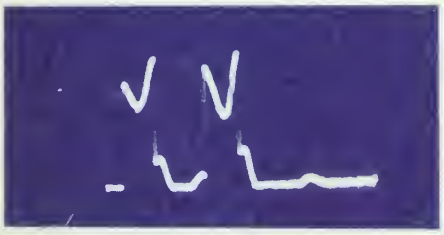

Photo. 18

U-State Current

Photo. 19

$\overline{U}$-State Current

Photo. 20

V-State Current

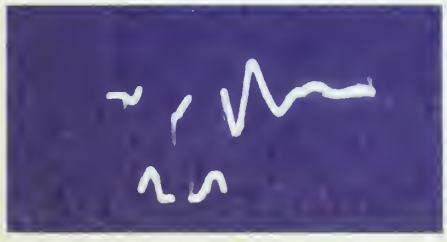

Photo. 21

$\overline{V}$-State Current

Note: Currents obtained using 0.5 ohm resistances in series with each motor stator winding.